AALBORG UNIVERSITY

Department of Health Science and Technology
Fredrik Bajers Vej 7D
9220 Aalborg Øst
Danmark

Title:
Modeling the Anatomical Differences in Human Lungs

Theme:
Biomedical Engineering and Informatics

Project Period:
10th semester, summer 2011

Project Group:
ST 11gr1086f

Group Participants:
Firas Nema Amin

Supervisor:
Dan Stieper Karbing

Copies: 2

Pages: 102

Appendix: 1

Finished 1st. of Jun, 2011

Synopsis:

Understanding the lung mechanics and gas exchange in healthy human lungs might be a step forwards in the way of understanding diseased lungs. One way to do that is by modeling the entire lung including the effect of gravity on distribution of ventilation and perfusion down the lungs. However, gravity has been estimated to cause a minor effect on perfusion distribution. The aim of this study is to use a model of perfusion designed by Mogensen et al. (2010) to investigate the hypothesis that anatomical differences in the lungs have the major effect on perfusion distribution down the lungs. To be able to answer this hypothesis, the study has implemented two anatomical gradients, namely length and number of capillaries surrounding the alveoli. By adjusting these gradients, the model is calibrated to fit an experimental data measured by Jones et al. (2001) describing distribution of perfusion in supine position. The hypothesis is then investigated, experimenting the perfusion distribution *In silico* in prone posture to evaluate the effect of the anatomical difference on distribution heterogeneity in the lungs. The result of the experiment is in agreement with studies suggesting that the distribution pattern of pulmonary perfusion is due anatomical differences in the lungs.

Preface

This report is the result of my project work during my 10th semester of Biomedical Engineering and Informatics at Aalborg University. The report was elaborated in the period from February 5th. 2010 to June 1st. 2011.

The primary purpose of this project is to evaluate the effect of anatomical differences in the lungs on distribution of perfusion, which might help understand the mechanism of matched ventilation/perfusion ratio. The report is addressed to students at the same educational level, supervisor, and people of the similar qualifications in the Public Health Sector.

References are stated according to the Harvard-method, by which a citation can be shown, for instance, as [Glenny et al., 2001], where the author's name and the publishing year are presented. The citation is displayed in the list of bibliography, as well. Citations prior to a full stop only refers to the last sentence. However, if a citation follows directly after a full stop, it refers to a paragraph or a section.

Firas Nema Amin

Contents

Part I

Introduction and Analysis

Chapter 1

Introduction

Patients admitted to intensive care units often suffer from acute respiratory failure and need acute respiratory support by mechanical ventilator to maintain sufficient gas exchange in their damaged lungs. In case of acute lung injury (ALI) or its severe form, respiratory distress syndrome (ARDS), mechanical ventilation has been proven to reduce patients' mortality and their recovery time [Lumb, 2005]. However, the answer of "what are the optimal ventilator settings for enhancing the patients' surviving?" is still unknown. To understand the domain of this problem, pathophysiology of the lungs, incidence and mortality of ALI/ARDS and mechanical ventilation therapy will be described. Subsequently, the chapter will present results of some important trials that has been conducted investigating this issue. The chapter will thereafter demonstrate what has been done in order to understand the lung mechanics in health and disease. Finally, the chapter will end with summary.

1.1 Pathophysiology

The terminology ALI describes a distinct severity form of a parenchymal lung syndrome and represents a wide range of severities, from short-lived dyspnoea to the most severe form, ARDS [Lumb, 2005]. Thus, it was not obvious, where the boundary between ALI and ARDS was until a clear definition by American-European Consensus Conference was agreed upon in 1994 to remove any confusion arisen as a result of different diagnostic criteria. The confirmation of ALI and ARDS diagnosis requires four criteria [Lumb, 2005, McCance and Huether, 2006]:

1. Acute onset of respiratory failure (the oxygenation is impaired).
2. A chest radiograph with bilateral pulmonary infiltrates.
3. Severe hypoxemia that is determined using the ratio Pa_{O_2}/FI_{O_2}, the ratio of partial pressure of oxygen in the patient's arterial blood to the fraction of oxygen

in the inspired air. The ratio in ALI $\leq$ 300 mmHg; in ARDS the ratio $\leq$ 200 mmHg.

4. Pulmonary artery wedge pressure $\leq$ 18 mmHg in order to exclude pulmonary edema induced by cardiogenic related causes.

In general, patients who develop ALI/ARDS are already hospitalized to be treated for other medical problems. ALI and ARDS are both syndromes that develop in stages and are resulted from very different causes. The syndrome may start when an injury to the alveolocapillary membrane causes pulmonary edema. When the alveolocapillary membrane is injured, the permeability is increased. Increased alveolar permeability is a sign of ALI/ARDS, allowing fluid, proteins, and blood cells to leak from the capillary bed into the interstitial space and alveoli. The result is edema and hemorrhage which impair alveolar ventilation. The damage may occur directly or indirectly. Whether the damage occurred directly or indirectly the inflammatory response of the lungs is massive. Direct damage can result from e.g. inhalation of toxic gases, whereas indirect damage can be caused by chemical mediators released in response to systemic disorders, as with sepsis and trauma. [McCance and Huether, 2006]

1.2 Incidence and mortality

It is believed that the widely varying estimates of incidence in the past are due to the lack of accepted definition of ALI and ARDS. Nevertheless, there is a substantial agreement that ALI/ARDS can cause an overall mortality of 50% in the intensive care units. [Lumb, 2005]

In USA alone, it is estimated that the syndromes can affect 200,000 to 250,000 people, annually, with complications in over 30% of all admissions to the intensive care units. [McCance and Huether, 2006]

In the year 2009, a comprehensive literature review of major studies was carried out to investigate whether the incidence of mortality among patients with ALI/ARDS was decreasing [Phua et al., 2009]. The studies searched multiple databases (MEDLINE, EMBASE, CINHL, Cochrane CENTRAL) for prospective observation studies or randomized controlled trials that enrolled more than 50 patients with ALI/ARDS and reported mortality in the period between 1984 and 2006. The study involved 18,900 patients with mean age of 51,6 years. The study conclusion was no considerable decrease in mortality had occurred since the consensus definition of ALI/ARDS was published in 1994. The study also reported that ALI/ARDS causes mortality of 35-40% for the randomized control trials. Additionally, the study highlighted the lack of adequate number of effective treatments for ALI/ARDS. [Phua et al., 2009]

1.3 Ventilator-induced lung injury

Mechanical ventilation is the usual intervening tool to provide therapy to patients with ALI/ARDS, because it can help recruit collapsed alveoli and improve pulmonary gas

exchange. Unfortunately, finding an appropriate ventilation setting is not an easy task for patients with ALI/ARDS due to the so-called ventilation induced lung injury (VILI); the term is utilized to describe lung injury that results from mechanical ventilation. [Verbrugge et al., 2007]

In clinical practice, damage associated with mechanical ventilation can rarely happen in normal lungs; it may only cause a problem when the patient is continually ventilated with high airways pressure or large tidal volume [Lumb, 2005]. However, this is not the case as may be observed in patients with ALI/ARDS because of their heterogenous lungs. For this group of patients, high pressure can over-extend normal alveoli resulting in generation or worsening lesions of alveolocapillary membrane [Lumb, 2005, Rotta, 2006, Chiumello et al., 2008]. Figure 1.1 illustrates three types of alveoli that could be presented in the lung tissue of patients with ALI/ARDS: normal alveoli, recruitable alveoli, and collapsed alveoli (consolidation tissue).

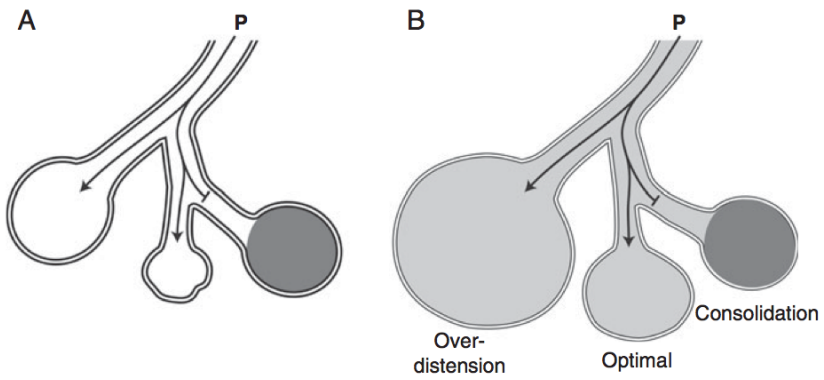

Figure 1.1: *Schematic representation of heterogeneity within the lung tissue of patients with ALI/ARDS at the onset of inspiration (A) and at the end of inspiration. Pressure (P) acting on lung tissue produces different effects. During inspiration, alveoli can be either collapsed (consolidation), optimal inflated, or over-inflated. [Soni and Williams, 2008]*

During mechanical ventilation, high pressure inside the lung at the end of inspiration may open recruitable alveoli, but over-extend normal alveoli. Lung consolidation tissue contains alveoli that are unlikely of impossible to recruit.

Furthermore, mechanical ventilation can cause a shearing injury which happens when recruitable alveoli are opened and closed repeatedly [Girard and Bernard, 2010].

The lung injury may first appear at one lung, but then it may spread rapidly affecting the other lung [MacIntyre, 2000]. The distribution of lung injury is heterogeneous, which results in unpredicted gas distribution when applying mechanical ventilation for patients with ALI/ARDS [Lumb, 2005].

1.4 Study-based indications

The realization that the ventilator may damage the lungs has led to change in ventilation settings in order to protect the lungs [Girard and Bernard, 2010]. This change has led to some reduction in mortality of ALI/ARDS patients [Verbrugge et al., 2007]. However, controversy continues in the literature regarding the optimal ventilation settings in order to minimize the risk of VILI and to properly secure oxygenation. Numerous studies have experimented with different pressure/volume ventilator settings attempting to identify the most appropriate one that can improve mortality outcomes of ALI/ARDS patients, of these studies [Amato et al., 1998, MacIntyre, 2000]. The objective was to recruit collapsed alveoli as a means of obtaining "full" lung contribution in gas exchange

The ARDS Network study (2000) has investigated this hypothesis using either low or high tidal volume plus positive end expiratory pressure (PEEP). The study has shown reduction in the mortality of patients that were ventilated with low tidal volume. In addition, the study has shown an increase in the number of days without use of ventilator in the low tidal volume group. [Brower et al., 2000] A few years later, An animal study has shown the importance of utilizing PEEP in protecting rat lungs (n=40) from damages that may happen due to cyclic opening and closing of the lungs. However, the PEEP level has no remarkable effect on the death rate reported in an ARDS Network study (2004) in which patients (n=549) were randomized to receive low tidal volume with either low or high PEEP level [Brower et al., 2004]. Similar studies have been carried out to find the optimal PEEP level when patients were ventilated with low tidal volume; these studies also failed to find any significant difference between low and high PEEP groups [Mercat et al., 2008, Meade et al., 2008].

The current understanding for lung mechanics is based on the above mentioned studies, among others. However, inconsistency between the results of these studies may indicate a lack of understanding the mechanical behavior of the lungs during mechanical ventilation. This has resulted in attempts for mathematically modeling pulmonary ventilation and perfusion through the lungs to better understand the lung mechanics. In the following section, benefits of using mathematical physiological models will be explained, and a number of mathematical models of the lungs will be reviewed.

1.5 Lung modeling

Mathematical models have been designed for providing better understanding of the mechanics of the respiratory system in health and disease. The advantages of applying mathematical models can be summarized in three points. First, because a useful model is designed and based on many experimental studies, it can provide a mechanism for the interpretation of existing data. Second, the process of including different experimental data in one single framework can help highlighting gaps in our understanding of the physiological system. Third, a well-designed model that can fit reality makes it possible to test new hypotheses. [Kansal, 2004].

When modeling the lungs, inhomogenous distribution of ventilation and perfusion through the lungs should be considered which characterizes diseased lungs (see section 1.3), but also healthy lungs to a certain extent [Galvin et al., 2007]. It is known that gravity causes a hydrostatic gradient through the lungs and result in inhomogeneity [West, 2002]; gravity was regarded as the main contributor to heterogeneity when modeling healthy lung [West et al., 1964, Hughes et al., 1968].

Furthermore, designing a mathematical model that can describe relationship between lung ventilation and perfusion during mechanical ventilation is desirable to estimate the effect of PEEP on perfusion distribution and, thus, gas exchange through the lungs [Walther et al., 2005].

The following section will review some mathematical models that have been built to describe lung mechanics in healthy and diseased lungs.

1.5.1 Physiological models

Different lung models of varying complexity have been designed to describe lung mechanics, e.g. [Dale et al., 1980, Wilson and Bachofen, 1982, Hickling, 1998, Venegas et al., 1998, Liu et al., 1998, Steimle et al., 2010, Mogensen et al., 2010]

Modeling the lungs in disease, Hickling (1998) constructed a comprehensive mathematical model of the ARDS lung to investigate the impact of changing alveolar opening pressure and PEEP on the slope of the pressure-volume curve. The lower and the upper inflection points and their relationship on alveolar stability was examined as well. The model described the lung as it was divided into number of horizontal slices simulating heterogeneity due to increasing gravitational superimposed pressure in each slice, from dependent to nondependent lung regions. However, the model neglected the effect of chest wall as well as the lungs were modeled to collapse at zero transmural pressure. In addition, Hickling's model failed to reliably estimate optimal ventilation settings from the simulated pressure-volume curve.

However, understanding lung mechanics in normal lungs may help in understanding the lung mechanics in disease. Dale et al. (1980) formulated a mathematical model of the normal alveolus utilizing finite element theory to simulate the pressure-volume relationship. The model included both the material properties of the alveolar fibrous supporting network existing in the alveolar structure and alveolar geometry. However, the model described a single component of the lungs in high details neglecting the heterogeneity within the lungs. Similarly, Wilson and Bachofen (1982) constructed a detailed mechanistic model for the alveolar duct which described alveolar openings as a network of intersecting helices. This model was not intended for use in clinical practice. Venegas et al. (1998) designed physiological model describing the complete respiratory system of the lung. The model was empirically formulated by a sigmoidal equation of the static P-V curve. Thus, it cannot be used to simulate the non-uniform distribution of ventilation and perfusion down the lungs, which is essential for understanding the link between lung mechanics and gas exchange.

Liu et al. (1998) designed a nonlinear model in which lung mechanics, pulmonary blood flow, and gas exchange were considered. However, the model is built as a lumped single-compartment model neglecting inhomogeneity within the lungs.

A comprehensive model of ventilation was designed by Steimle et al. (2010) in which the lungs were described as stratified making simulation of local ventilation possible at different layer depths of the lungs. This model combined lung mechanics and distribution of ventilation in the healthy lungs. The model contained different important aspects of: the alveolar geometry; chest wall pressure; alveolar surface pressure due to surfactant activity; pressure caused by elasticity of pulmonary tissue; pressure related to hydrostatic effects of the pulmonary tissue and blood. However, validation of the ventilation model showed poor fit to an experimental data by [Brudin et al., 1994], which measured in healthy human subjects in supine posture, see Figure 1.2. The model overestimated the non-dependent lung region and was unable to describe the trend of the experimental data, generally.

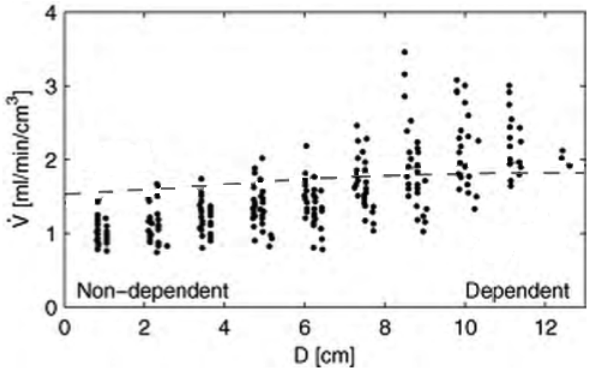

Figure 1.2: *Simulation of ventilation model (broken line) against an experimental data by [Brudin* et al.*, 1994] for healthy human subjects in supine position. The model simulation overestimated the non-dependent lung zone. Besides, the simulation was incapable of describing the trend of the experimental data. The figure modified from [Steimle* et al.*, 2010]*

Based on Steimle's model, Mogensen et al. (2010) formulated a physiological model of perfusion enabling simulation of the influence of lung volume, airway pressure, and hydrostatic effects on pulmonary blood flow at different lung depths. The model incorporated important aspects of: capillary geometry; elasticity of capillary wall; pressure at the pulmonary artery; the chest wall effect; blood viscosity; the influence of gravity due to hydrostatic effects of the lung tissue and the blood during breathing, going from the non-dependent to the most dependent layer of the lungs. Furthermore, the model simulated pulsatile blood flow with an increasing blood perfusion down the lungs. Nevertheless, the models' simulations of perfusion showed a poor fit to an experimental data by [Jones et al., 2001]. Figure 6.1 presents distribution of perfusion (solid line) in healthy human subjects in supine position down the lungs from non-dependent to dependent lung regions. The pulmonary capillary perfusion was normalized to mean perfusion.

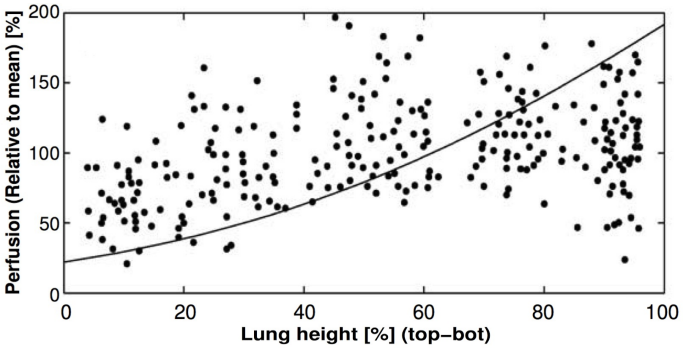

Figure 1.3: *The figure shows simulation of the blood perfusion through the lung (solid line) and experimental data by Jones et al (2001). The simulation showed a poor fit to the experimental data. The figure is modified from [Mogensen* et al.*, 2010]*

The trend of the experimental data in Figure 6.1 shows a reduction in pulmonary perfusion at the ventral (top) and dorsal part (bottom) of the lungs, and increased perfusion towards the middle of the lungs. Although the model described the heterogeneity of perfusion due to effect of gravity, the model simulation underestimated the total capillary perfusion compared to the experimental data. In addition, the model was neither able to simulate the dependent nor the nondependent regions of the lungs. This may indicate that there are other influential factors than gravity, causing this pattern of heterogeneity.

The following section will summarize the problem presented in this chapter resulting in an initial problem to be analyzed in the following chapters.

1.6 Initial problem

Acute lung injury and acute respiratory distress syndrome are terms used to describe a type of pulmonary injury which may occur from wide diversity of causes or associated conditions. Resent studies have shown that the level of mortality of patients with ALI/ARDS is not decreasing as been previously believed. Nevertheless, an appropriate ventilation setting can improve the patients' mortality due to, perhaps, avoiding the number of opening and closing of the alveoli, and over-inflating the alveoli. Many studies have been carried out to find optimal ventilation setting for the patients with the ALI/ARDS. However, disagreement regarding interpreting the results of these studies continues in the literature which may indicate a lack of understanding of how tidal volume and PEEP affect lung mechanics. A step toward understanding the lung mechanics and gas exchange in disease can be perfumed by modeling normal lungs. Numerous models has been designed simulating either single compartment with heigh details or complete system of healthy lungs neglecting heterogeneity of perfusion distribution. Designing a comprehensive physiological mathematical model of ventilation and perfu-

sion describing inhomogeneity within normal lungs might lead to understanding lungs disease.

Mogensen et al. (2010) formulated a model of perfusion basing on a model of ventilation prepared by Steimle et al. (2010) including different important aspects of pulmonary perfusion. This study will be focused on the perfusion model by Mogensen et al. (2010). The perfusion model described the lungs as been divided into horizontal layers, enabling simulating heterogeneity of blood flow due to gravity alone. Nevertheless, validation of the perfusion model against experimental data by Jones et al. (2001) shows underestimation of pulmonary perfusion in nondependent lung region and overestimation of the dependent lung regions. Therefore, the following initial problem will be studied in the following chapters:

Which effects can influence distribution of blood flow in healthy human lungs?

Chapter 2

Pulmonary Perfusion

The aim of this chapter is to investigate what mechanism that can cause heterogenous distribution of perfusion in normal human lungs, and what the distribution profile is. To achieve that, a number of studies will be reviewed describing their results.

2.1 Mechanisms affecting perfusion

Number of mechanisms can be a factor in perfusion heterogeneity in the lungs:

Active mechanisms contribute to matching ventilation and perfusion, e.g. hypoxic pulmonary vasoconstriction [Glenny and Robertson, 2011]. The effect of the active mechanisms were investigated by [Arai et al., 2009, Robertson, 2009, Glenny and Robertson, 2011] who reported that they cause a minor or negligible role in distribution of blood flow in the normal human lungs. However, active mechanisms are significant to consider under pathologic condition. [Glenny and Robertson, 2011]

Passive mechanisms can be the geometry and branching pattern of pulmonary airways and vascular tree, and the vertical gradient due to gravity [Glenny and Robertson, 2011]. Knowing that gravity influences the distribution of ventilation and perfusion through the lungs has led to suggestion of changing posture in patients with ALI/ARDS to eliminate compression of the dependent region of the lungs and enhance gas exchange. [Tobin and Kelly, 1999]. In general, various studies have shown altering in perfusion distribution when changing from supine to prone position, such as [Nyrén et al., 1999, Mure and Lindahl, 2008], although other findings that showed no significant altering in perfusion in the prone posture [Amis et al., 1984, Jones et al., 2001, Musch et al., 2002]. The variability of pulmonary blood flow due to gravity was estimated by [Jones et al., 2001, Glenny et al., 1999] to cause only 10-40%. This was done by fitting a linear regression model to an experimental data measured in healthy human subject in supine and prone posture, calculating the goodness of fit. This leaves approximately 60-90% of blood flow heterogeneity to be explained by other passive mechanisms, e.g. pulmonary vascular geometry and branching structure in the lungs,

which were suggested by [Glenny et al., 1991,Glenny et al., 1999,Glenny and Robertson, 2011] to have a great effect on distribution of perfusion in the normal lungs.

2.2 Perfusion heterogeneity

Distribution of pulmonary perfusion has been researched repeatedly by different studies, e.g. [Amis et al., 1984,Hakim et al., 1987,Hakim et al., 1988,Levin et al., 2001,Glenny et al., 1999, Glenny et al., 1991, Glenny et al., 2000], showing a persistent pattern of heterogeneity through the lungs. Some of these studies are chosen to be reviewed due to their important results in describing blood flow distribution.

The study by Hakim et al. (1987) using single photon emission computerized tomography of the lungs was conducted to examine the three dimensional distribution of pulmonary blood flow in healthy human subjects. The study showed concentric pattern of radioactivity in the center of the mid-coronal slices the lungs that gradually decreased in activity from the center to the periphery of the subjects in the supine posture. [Hakim et al., 1987] Perfusion image of a lung slice is shown in Figure 2.1

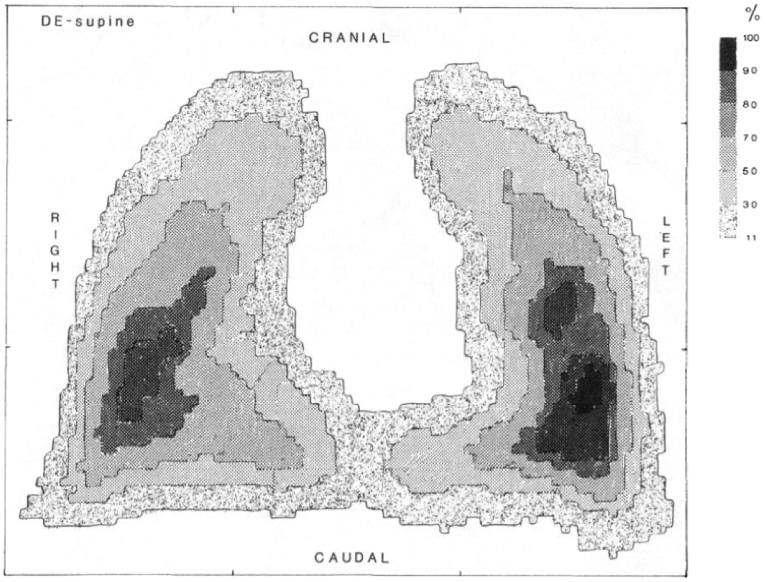

Figure 2.1: *A typical tomographic image of mid-coronal slice illustrating the distribution of the blood flow in the horizontal plane of the subject in the supine posture. The image manifests that there is a gravity independent gradient governing the distribution of blood flow. In this slice, 10% of maximal activity was removed for background and edge scatter; isoflow region was divided into 6 shades as presented in the scale from 11-100% (11-30;30-50;50-70;70-80;80-90;90-100). The scale describes a [Hakim* et al.*, 1987]*

Hakim et al. (1987) also investigated the distribution of blood flow in the sagittal planes (gravity dependent plane) which manifested a similar pattern of concentric gradient in

activity. The distribution of flow in the vertical plane (gravity dependent) was almost comparable to the horizontal distribution. This may suggest that the pulmonary blood flow is spatially stratified with marked gradient from the center to the periphery in all directions. Figure 2.2 depicts isoflow regions of a typical tomographic image when a sagittal slice through the middle of the right lung is taken. [Hakim et al., 1987]

Another study by Hakim et al. (1988) was conducted to investigate the effect of body posture on spatial distributing of blood flow using Single-photon emission-computed tomography. The study examined six anesthetized healthy dogs, two of which were in the supine posture, two in the prone position, and two suspended in the upright position. The study demonstrated isogravitional perfusion heterogeneity, independent of body position, with blood flow in the pulmonary central region 10 times that in the periphery. Even though perfusion inhomogeneities were presented independent of gravity, the central region with the highest perfusion was closer to pulmonary dependent region which suggests that the gravity had some influence on the final distribution. Halkim et al. (1988) suggested that anatomical differences in the lungs can be an explanation to this heterogeneity, e.g. branching of the vascular vessels. [Hakim et al., 1988]

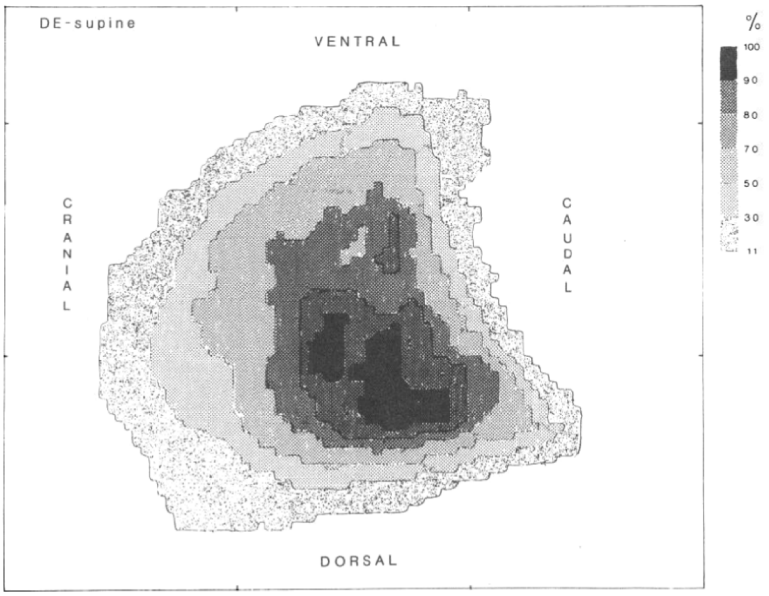

Figure 2.2: *A typical tomographic image of sagittal slice through the middle of the right lung in one subject. In this slice, 10% of maximal activity was removed for background and edge scatter; mapping the isoflow region was divided into 5 shades as presented in the scale [Hakim* et al.*, 1987]*

Levin et al. (2001) studied pulmonary transit time, blood volume, and perfusion in isogravitational and gravitational-dependent planes, using an ultrafast MR sequence. Measuring of changes in signal intensity during first pass of intravascular contrast through pulmonary circulation was conducted. Six healthy human subjects were im-

aged (three males and three females) along coronal plane, where six different regions of interest were chosen in each lung apex and base, for a total of 12 measurements in each subject's lung while subjects in supine posture. From the quantified data, mean transit time, blood volume, and blood flow were computed. The study demonstrated a significant gradient in transit time, with faster times in the lung apex, as well as a significant decrease in blood volume in the lung apex in comparison with the lung base. [Levin et al., 2001] Figure 2.3 shows the results of the study where blood gradient between the lung apex and base is manifested in the six subjects.

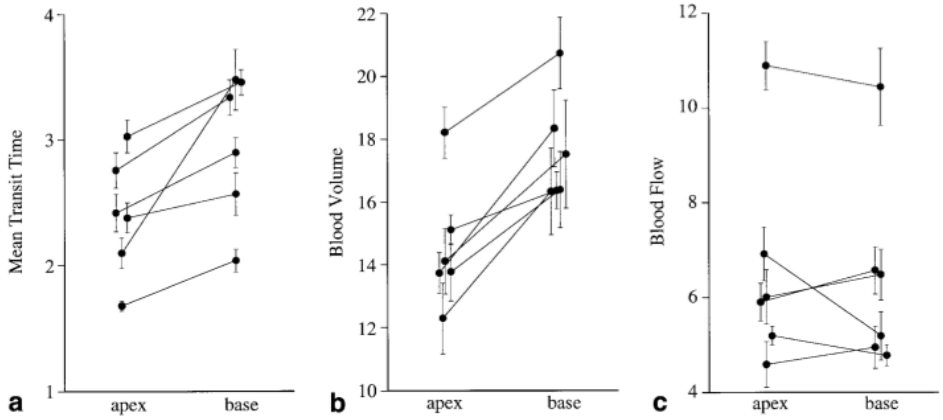

Figure 2.3: *Experimental data showing regional differences between the apex and the base of healthy human lungs for mean transit time (a), blood volume (b), and blood flow (c). For each subject the data were presented as mean with standard error of the mean. The means of the data from the apex and base of the lungs were connected by a solid line. The data of blood volume and blood flow of each region of interest were plotted with arbitrary units, and were given relative to lung artery for each subject. The mean transit time computed in seconds from the pulmonary artery to region of interest. [Levin* et al.*, 2001]*

Studying gravitational dependent and nondependent portions of the lungs, differences between the lung central portions and the lung periphery were examined. Measurement were acquired in a off-midline, sagittal plane through the right lung, while subjects were in both supine and prone posture. The study showed a significant decreases in blood flow and blood volume towards the lung periphery. The study concluded a presence of radial distribution of perfusion. Figure 2.4 shows the regional distribution of blood flow from lung central segment to the periphery [Levin et al., 2001]. The author provided no explanation for the high variation in measurements between the six subject.

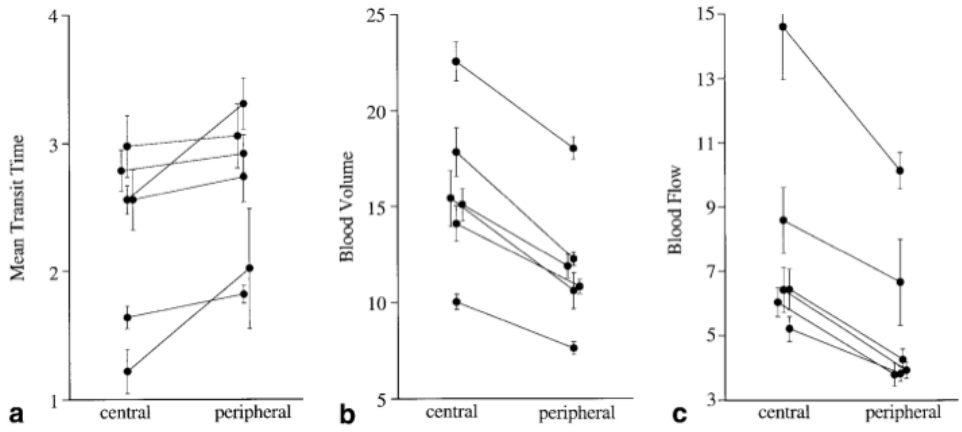

Figure 2.4: *Experimental data presenting regional differences between the center and the periphery of the lung of healthy human lungs for mean transit time (a), blood volume (b), and blood flow (c). For each subject the data were presented as mean with standard error of the mean. The data means from the center and periphery of the lungs were connected by a solid line. The data of blood volume and blood flow of each region of interest were plotted with arbitrary units, and were given relative to lung artery for each subject. The mean transit time were computed in seconds from the pulmonary artery to region of interest. [Levin* et al.*, 2001]*

Glenny et al. (1991) re-evaluated the effect of gravity on distribution of perfusion. The coworkers studied pulmonary distribution using seven dogs in supine and prone postures. The study quantified blood flow under zone 3 conditions to assess a linear gravitational model of blood flow distribution. The experimental was conducted by injection of radiolabled microspheres in both positions. The study showed marked flow inhomogeneity inside isogravitational planes with coefficient of variation (CV=100*SD/mean, used as a measure of heterogeneity) of 42.5 %. In addition, heterogeneity was also shown in gravitational plane with coefficient of variation of 44.2 % in supine and of 39 % in prone positions. Although the gravitational model states that perfusion should be negatively correlated when measured in the supine and the prone positions, the study showed that in both positions the perfusion was positively correlated. Figure 2.7 presents an experimental data from one dog in the supine position, the perfusion heterogeneity in each isogravitional plane indicated by the standard deviation bars. These heterogeneities can not be explained by hydrostatic pressure. [Glenny et al., 1999]

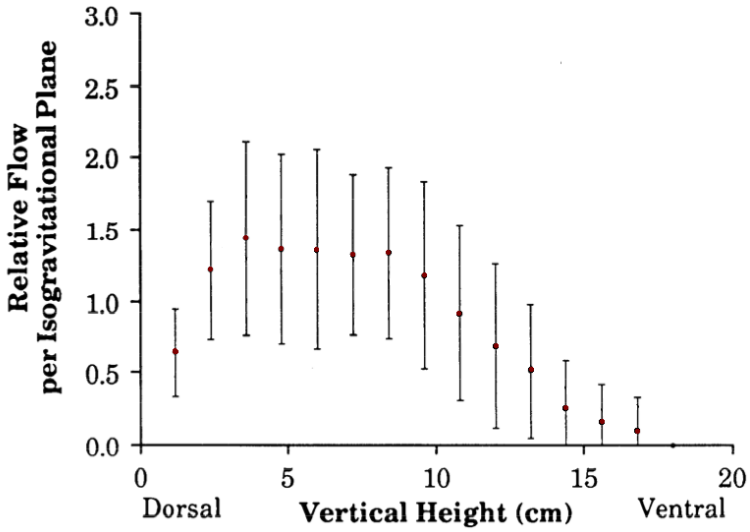

Figure 2.5: *Experimental data illustrate regional variation of blood distribution in the isogravitional plane as a function of vertical height for a dog in the supine posture. Perfusion within isogravitional planes presents heterogeneity which is illustrated with SD bars.The figure is modified from [Glenny* et al.*, 1991]*

The experimental data shows a vertical gradient of perfusion, going form zone 1 (non-dependent region) passing through zone 2 and zone 3. However, reduction in blood flow is presented in the most dependent lung region ("zone 4") which may be explained by other factors than gravity such as anatomical differences in pulmonary vascular tree between lung regions.

2.2.1 Perfusion at different gravitational conditions

Pulmonary perfusion has been perviously studied by [Glenny et al., 1991] showing increased distribution of blood flow in the most dependent lung region when gravity was nullified. Some years latter, [Glenny et al., 2000] investigated perfusion heterogeneity in the lungs during weightlessness and increased gravity on six juvenile pigs, which were injected with fluorescent microspheres to the pulmonary circulation during supine and prone postures at different gravitational conditions. Thereafter, the lungs were removed and subdivided into pieces of approximately 2 cm^2, in which perfusion were measured for the different conditions. The study revealed a minor effect of gravity on pulmonary blood flow suggesting that the pulmonary vascular tree is the major determinant of regional distribution of perfusion in these animals. In Figure 2.6, the experimental data illustrates vertical distribution of perfusion in one lung during the supine posture and conditions of 0-, 1-, and 1.8-G. Increasing gravitational forces results in steeper vertical gradient of perfusion down the the lungs. It should be noticed that decreased perfusion in the dependent lung regions (zone 3 and 4) persists during weightlessness.

Linear model were fitted to these data excluding the most dependent lung regions was proposed to investigate the effect of pulmonary vascular structure and hydrostatic gradient.

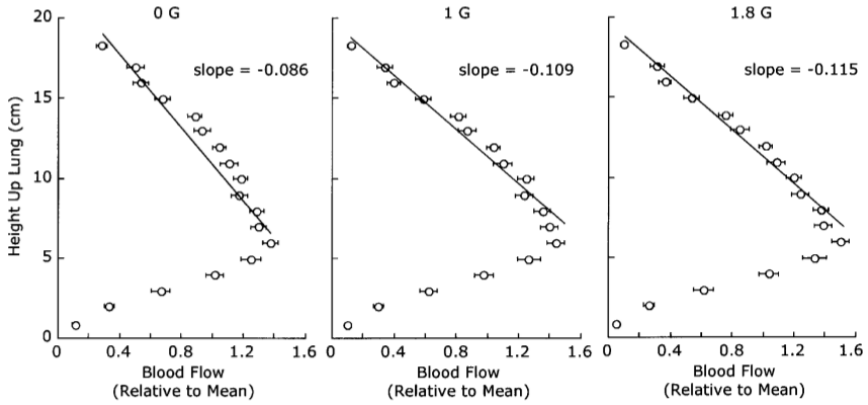

Figure 2.6: *Experimental data showing vertical distribution of perfusion for one pig in the supine position during 0-, 1-, and 1.8-Gravity. Linear model were fitted to these data where "zone 4" was excluded. Slope of the linear model were calculated from a least squares. Data were plotted as means±SE. Decreased perfusion in the dependent regions (zone 3 and 4) remaina in all gravitational conditions. [Glenny* et al.*, 2000]*

2.2.2 Perfusion in the supine vs. prone postures

Various studies have been carried out to investigate distribution of perfusion in the supine and the prone position showing either enhancing [Nyrén et al., 1999, Mure and Lindahl, 2008] or non significant improving [Amis et al., 1984, Jones et al., 2001, Musch et al., 2002].

[Prisk et al., 2007] examined the effect of changing posture on regional blood flow using MRI technique. The study was carried out on six healthy human in the supine and prone postures. For these subjects, data were obtained in three nonoverlapping 15-mm sagittal slices of the right lung. The slices were from central, middle, and lateral lung covering most of the right lung. The slices were additionally subdivided into vertical regions: anterior (nondependent), intermediate, and posterior (dependent). Measuring the entire lung density showed no difference between supine and prone positions. However, increase in lung density in the anterior zone was less than decrease in the posterior zone when when subject in the prone position. Perfusion was measured in milliliter per minute per cubic centimeter. Figure 2.7A and B represent distribution of blood flow from one subject in supine and prone postures for the three sagittal lung slices, respectively. Figure 2.7C-E shows lung perfusion for central, middle, and lateral slices in supine (dashed) and prone (solid) postures. The perfusions were shown as mean; the shaded zones present mean ± SD. The experimental data present a pattern

of blood flow distribution similar to that presented by [Hakim et al., 1987] showing central-to-peripheral gradient in blood flow in all directions, with greatest blood flow in the center of lateral direction as well as in the anterior-to-posterior directions.

Investigating the compressive effect on both perfusion and ventilation is significant in order to understand pulmonary gas exchange in the supine and prone postures. However, in the healthy human lungs, changing positions from supine to prone results in modest inhomogeneity of ventilation/perfusion ratio. [Prisk et al., 1994]. The next chapter will consider this issue in more details due to its importance in describing gas exchange through the lungs.

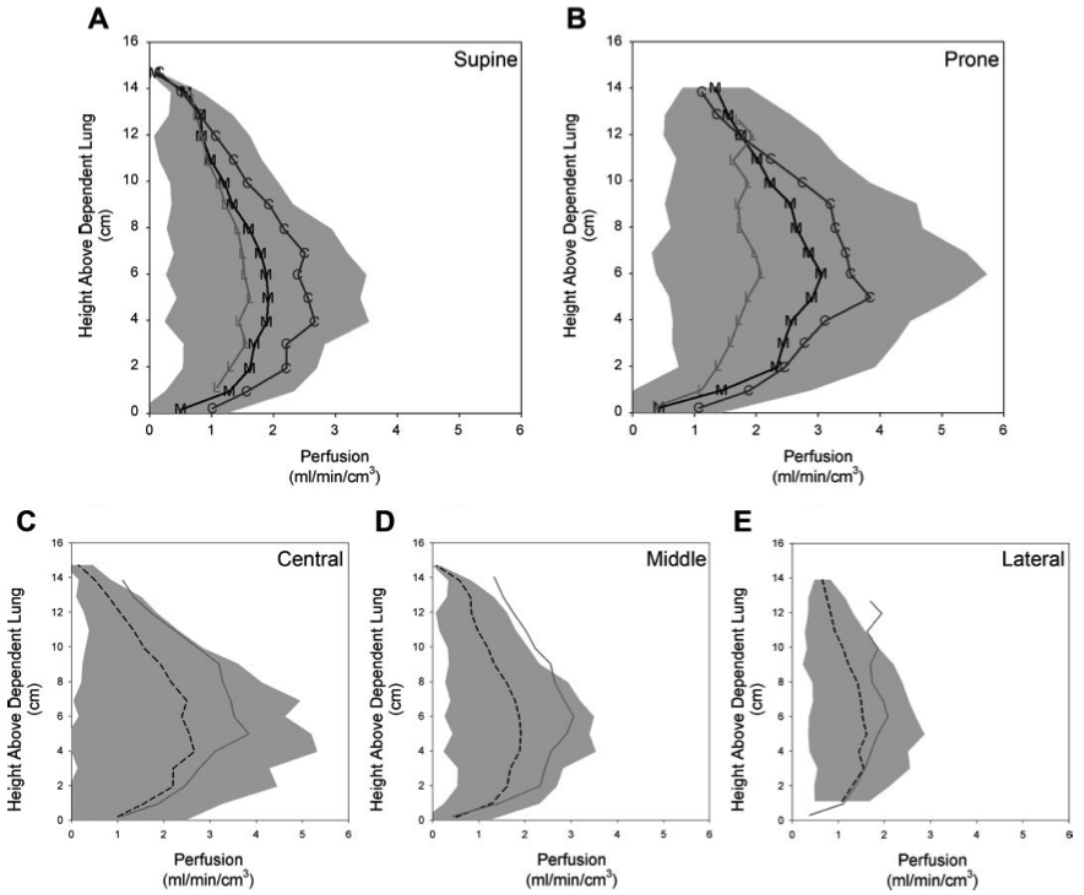

Figure 2.7: *Blood flow distribution as a function of lung heigh above dependent lung when subject in the supine (A) and prone (B) positions for the three sagittal slices: central (C), middle (D), and lateral (E). Lines represent the average lung blood flow; dashed and solid lines depict supine and prone postures, respectively. The mean pulmonary perfusion±SD is presented with shaded regions. Modified from [Prisk* et al.*, 2007]*

2.2.3 Modeling the gravity effect

Different factors affect ventilation, perfusion, and gas exchange in the lungs. The importance of gravity in determining the pulmonary perfusion and compression of lung parenchyma has been reported repeatedly [West et al., 1964, Hughes et al., 1968, Jones et al., 2001, West, 2002]. Distribution of the blood flow was described first by West et al.(1964) in terms of capillary resistance due to the hydrostatic pressure. West et al. (1964) suggested a physiological model of the lung where the lungs were subdivided into three vertical zones based upon the relation between the alveolar, artery, and venous pressures [West et al., 1964]. The gravitational model by West et al. (1964) is based on the following assumptions [Glenny et al., 1999]:

- Uniform distributions of blood flow within isogravitional planes
- There is a reverse relationship between regional blood flow and vertical distance from independent to dependent lung regions, independent of body position.
- The correlation between regional blood flow measured in the supine position and the same regional flow in prone positions should be negative.

The three zones model was modified by Hughes et al. (1968) where a forth lung zone was added below the lung's third zone. [Hughes et al., 1968]. However, the mechanism that effect distribution of perfusion in the forth zone is not clearly evident. A potential explanation of the mechanism for blood distribution in zone 4 might be anatomical differences due to capillary distribution. Figure 2.8 shows the lung zones where blood flow is distributed heterogeneously in the vertical direction through the lung.

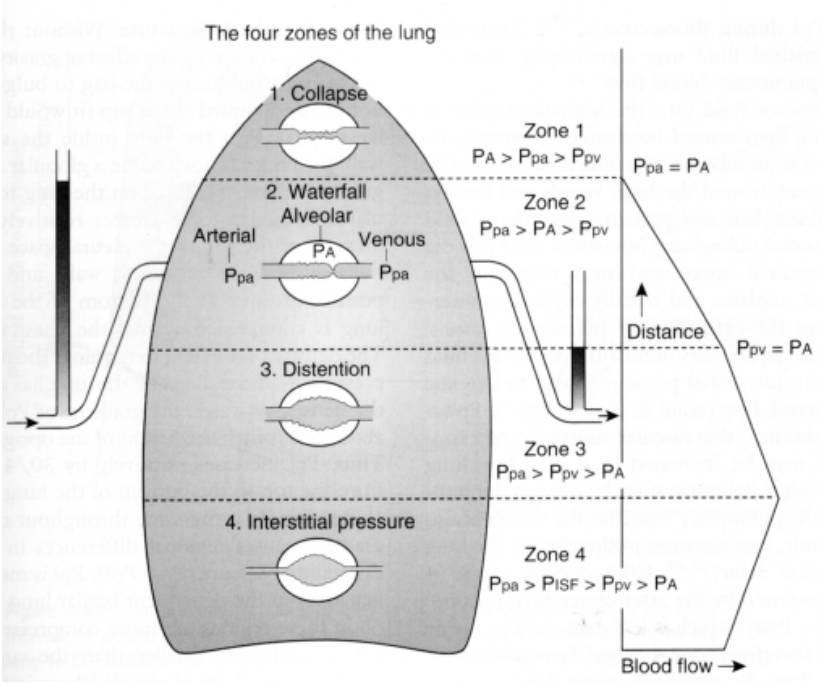

Figure 2.8: *The diagram shows lung zones as modeled by West et al. (1964) (1-3 zones) and altered by Hughes et al. (1968) by adding a fourth zone. The resistance in the different parts of the lung are believed to determine the blood flow distribution. The zone 1, no flow occurs because the capillaries are collapsed. At this zone, alveolar pressure P_A exceed pulmonary artery pressure P_{pa}. In zone 2, P_{pa} exceeds P_A which in succession is greater than the venous pressure. The flow in zone 3 depends on the arterial-venous pressure difference; the venous pressure exceeds alveolar, and flow intensifies with distance down the lung. Hughes postulated forth zone, where blood flow declines with distance towards the base of the lung probably due to increased interstitial pressure which reduces the radius of the large capillaries (extra-alveolar) in the lung.* [Hughes et al., 1968]

In zone one, the vessels are collapsed and closed because alveolar pressure exceeds arterial pressure; there is no flow through the capillary bed. The blood flow starts at zone two where the arterial pressure exceeds the alveolar; the arterial-alveolar pressure difference determines the blood flow since the alveolar pressure exceeds the venous. The behavior in this zone reassembles the so-called waterfall or Starling resistor. In zone three, the venous pressure exceeds the alveolar causing the flow to depend on the arterial-venous pressure difference, and blood flow becomes greater down this zone as a result of distensibility and recruitment of new vessels. In zone 4, Hughes postulated that the flow in the forth zone is reduced because of increasing interstitial pressure which narrows the radius of the extra-alveolar capillaries in the most dependent zone [Hughes et al., 1968].

Chapter 3

The Lung Anatomy and Physiology

Studying the structure and intensity of pulmonary capillaries surrounding the alveoli might be as important as the mechanical properties. This chapter reviews number of studies concerning capillary shape, length, relaxing radius, and elasticity of the alveolus.

3.1 The pulmonary circulation

The pulmonary circulation is a high-flow, low-pressure, and low-resistance system. In contrast to the systemic circulation, the resistance of the pulmonary circulation is low because of the shorter total length of the vessels and the distensibility and the large cross-sectional area of the arterioles. The pulmonary artery is more compliance and has relatively thinner wall than the systemic artery. Similarly, the pulmonary arterioles are thin-walled vessels which contain little smooth muscle compared with their counterpart in the systemic circulation. [Rhoades and Bell, 2009, Martini, 2005]

The pulmonary circulation resembles the entire systemic circulation in receiving all of the cardiac output, approximately 5 L/min in healthy human adult [Silverthorn, 2001]. That is, as much blood perfuses the lungs as the rest of the body at the same time interval. The main function of the pulmonary vascular system is to bring the blood from the superior and inferior vena cavae in contact with lung alveoli for gas exchange. In addition, the lungs also serve as a filter, metabolic organ, and blood reservoir. There is approximately 500 mL blood or 10% of the total circulating blood volume in the human body; approximately 75 mL of this amount is found in the capillaries where gas exchange occurs [Silverthorn, 2001], whereas the remainder is in the pulmonary arteries and veins. During hemorrhagic shock, the lungs can mobilize some of this blood to improve the cardiac output. [Rhoades and Bell, 2009, McCance and Huether, 2006, Silverthorn, 2001]

In addition, the lung is capable of redistribution of the blood in case of presence of hypoxia and absence of hypercapnia. This mechanism of constriction of pulmonary vessels reduces the blood flow with higher oxygen concentration to alveoli. The most

significant cause of pulmonary vessel construction occurs when alveolar partial pressure of oxygen (P_{AO_2}) is low; it is often termed hypoxic vasoconstriction (HPV). HPV can influence one lung portion (lobe) or the entire lung. Insufficient alveolar P_{AO_2} in one lung segment can cause the arterioles perfusing that segment to constrict, shunting blood to other, well-ventilated portion of the lung. This reflex enhances the pulmonary work by better matching the ventilation and perfusion. [McCance and Huether, 2006]

In the center of the lung lobule the pulmonary arteries branches following the same branching manner as the airways and bronchial arteries and then split beyond it. The pulmonary arteries taper in diameter as they travel through the lung tissue giving off smaller arteries that further divide into arterioles and finally capillaries just before the alveoli. [Martini, 2005]

3.1.1 Pulmonary microcirculation

Pulmonary capillaries are subdivided into three distinct groups: alveolar capillaries, corner capillaries and extra-alveolar capillaries. The resistance of these capillaries is affected by the pressure inside the alveoli. The minimal resistance for pulmonary capillaries is reached when pressure inside alveoli is at functional residual capacity (FRC). The pulmonary capillaries are described as follows [Lumb, 2005]:

- Alveolar capillaries lie in the wall between two bordering alveoli. The capillaries are more subjected to pressure due to alveolar inflation, they resist collapse by the intravascular pressure and flimsy septal fibrous tissue. The resistance in these capillaries is thus related directly to the lung volume.
- Corner capillaries are situated in the junction that connects three or more alveoli. In general, they are not affected by pressure due to lung inflation. In contrast, the capillaries may dilate at high lung volume and narrow at very small volume, possibly as a result of local hypoxic that surrounds the collapsed alveoli.
- Extra-alveolar vessels. An additional explanation for the increased vascular resistance is provided by these vessels. If large lung vessels are compressed at low lung volumes, this causes flow reduction in the dependent parts of the lung. This may result in changing the overall pulmonary vascular resistance.

Figure 3.1 is a scanning electron micrograph of the alveoli in heathy human lung, illustrating alveolar capillary networks. The alveolus is separated from neighbored alveoli by septa. The architecture of alveolar capillary network has an influence on its transport function and on biophysiological behavior of blood flowing through it. That is, for a given perfusion pressure, the hydrodynamic resistance of a capillary lattice decides the overall blood flow. Calculating the capillary resistance requires: number and length of capillary segments, alveolar capillary geometry (network arrangement), passive and active mechanism controlling capillary radii, and blood viscosity. [Pries et al., 1996]

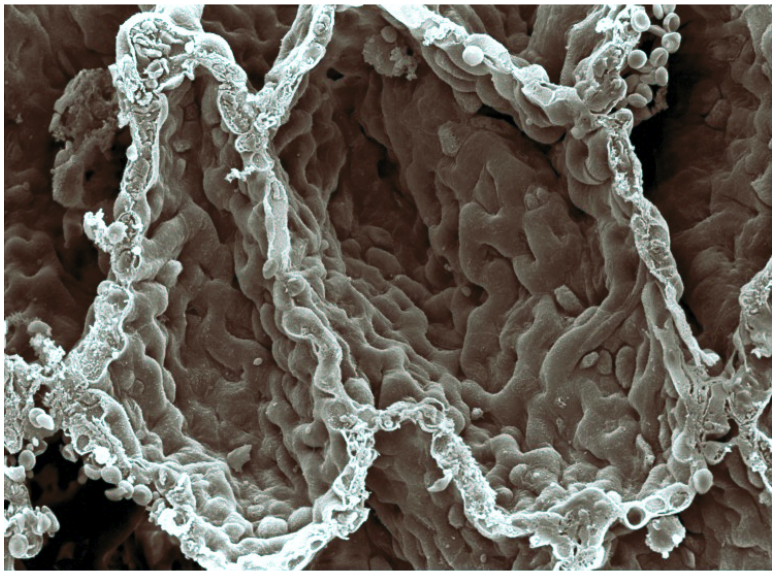

Figure 3.1: *Scanning electron microscopy showing cross sectional structure of the alveoli in healthy human lungs. Three neighbored alveoli are separated from each other by three septa. [Gregory and Marshall, 2003]*

3.1.1.1 Alveolar capillary geometry

Last decades, scanning electron microscopy has been extensively used to study pulmonary microstructures such as the structure of the alveoli. Applying this technique in studying the alveoli in rat, the acquired images reveal the structure of alveolar capillaries where they come together forming pentagonal rings [Schraufnagel and Schmid, 1988], see Figure 3.2. More than one alveoli can be supplied by only one capillary from which branches cover about 75 % of alveolar surface areas. The density of the capillaries on the pleural surface, around bronchioles, and in the bronchovascular bundle is lower than it is on alveolar sites [Schraufnagel and Schmid, 1988]. During ventilation, alveolar capillaries fold and unfold affecting the resistance to blood flow and thus ventilation-perfusion matching. Blood flow increases when inspiration begins from functional residual capacity because unfolding the capillaries enhance perfusion. Most expended alveoli receive more blood and ventilation, while already inflated alveoli at the beginning of the inspiration receive less blood flow because of narrowed alveolar capillaries. Folding may decreases perfusions during expiration, as well. [Hamid et al., 2005]

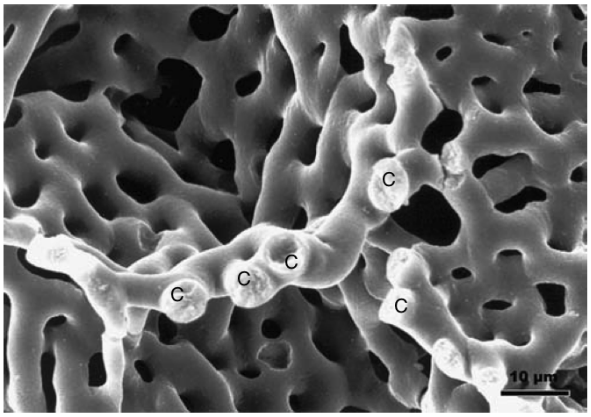

Figure 3.2: *Capillary structure of the cross sectional view of the alveoli in rat showing a cast of alveolar baskets. The image was taken using scanning electron microscopy. C: capillary. [Schraufnagel and Schmid, 1988]*

3.1.1.2 Capillary length

The network of alveolar capillary bed is constructed of complex, short, interconnecting capillary segments, see Figure 3.1. Every alveolus consists of approximately 1000 capillary segments, each of which was estimated to be about 8 μm in length [Voelkel and Rounds, 2009]. The total length of alveolar capillary bed can be computed by multiplying the number of segments by the length of each segment, which gives 8000 μm.

3.1.1.3 Blood viscosity

The viscosity of blood through a capillary segment smaller than 300 μm is positive correlated with capillary radius, because of the behavior of erythrocytes. When red blood cells travel through a capillary, they move over the center of the capillary causing parabolic velocity profile varies from zero at the wall to maximum in the center of the capillary. The viscosity of blood describes properties of blood in relation with the vessel at a given pressure. Measuring capillary viscosity in vivo is difficult, because it requires the simultaneous computing of: the pressure drop along a capillary segment, volume flow, length, and inner radius in that segment [Pries et al., 1996]. In addition, the computing of viscosity is sensitive to error in measuring the capillary inner radius. However, measuring the viscosity in vitro was carried out using glass tube at different radii; results of 18 studies were combined determining the viscosity profile as a function of tube radius, see Figure 3.3. [Pries et al., 1996]

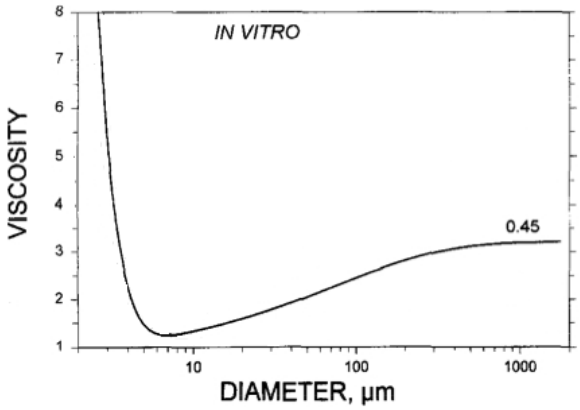

Figure 3.3: *The viscosity of blood varies as a function of capillary radius. The curve represents in vitro viscosity with hematocrit value of 45 % of adult human. The figure is modified from [Pries* et al.*, 1996]*

The viscosity profile was given for a hematocrit of 45 % in adult human. Hematocrit value is defined as the ratio of blood volume in a given region occupied by red blood cells to the volume of blood, and it is called hematocrit (adult human male, 45%) [Martini, 2005].

3.1.1.4 Capillary radius

The lung capillary is devoid of muscular control making it able to dilate in respond to capillary transmural pressure. [Sobin et al., 1972] measured the pulmonary capillary radius in cat showing that when capillary transmural pressure increased from 0.5-2.5 kPa, the capillary diameter increased from 5 to 10 μm.

3.2 Pulmonary Gas exchange

In the lungs, optimal gas exchange occurs when ventilation and perfusion distribute in the same proportion to one another, it will result in an optimal gas exchange [Lumb, 2005]. The ventilation to perfusion ratio (abbreviated to $\dot{V}/\dot{Q}$) is thus used to examine how well pulmonary gas exchange is. The quantities of ventilation and perfusion are normally measured in liters per minutes. Assuming that ventilation and perfusion are uniform through the entire lung, each individual alveolus would has $\dot{V}/\dot{Q}$ ratio of 0.8 l/min, a typical resting value approximated for the entire lung. The ratio is, however, not constant through the entire lung and its value varies from the apex to the base of the lung, varying from unventilated alveoli to unperfused alveoli. The alveoli with no ventilation will have a $\dot{V}/\dot{Q}$ ratio of zero, while the unperfused alveoli will have a $\dot{V}/\dot{Q}$ ratio of infinity. The unventilated alveoli will have P_{O_2} and P_{CO_2} values that are equivalent to those of mixed venous value, since the trapped air in the unventilated alveoli will equilibrate with the mixid venous blood and no more air reaching the alveoli.

Unperfused alveoli will have P_{O_2} and P_{CO_2} the same as the inspired gas because of no gas exchange will happen between alveoli and the surrounding capillary bad. [Lumb, 2005]

Chapter 4

Problem Statement

This chapter formulates the aim of this study on the basis of the problem introduced in the previous chapters. In addition, the chapter will describe the strategy for solving the problem statement.

4.1 Problem Statement

In the previous chapters, the motivation for this study has been described. Studies investigating distribution of perfusion in healthy human lungs in the supine and prone posture, and under nullified gravitational forces has shown persistence of perfusion heterogeneity with more pronounced blood perfusion in the posterior lung regions and less in the anterior regions. Some studies also have shown radial distribution of blood flow from the lung center to the periphery in all directions with center of perfusion closer to the dependent region.

Distribution of blood flow can be affected by active and passive mechanisms. The active mechanisms, e.g. hypoxic pulmonary vasoconstriction, contribute to redistributing of perfusion through the lungs. However, recent studies have reported a negligible effect of the pulmonary active mechanisms on distribution of blood flow in healthy human lungs, suggesting only passive mechanisms to be responsible for this heterogeneity, e.g. gravity, geometry and pattern of branching of pulmonary vascular tree [Arai et al., 2009, Robertson, 2009, Glenny and Robertson, 2011].

Unfortunately, non of the investigated studies determined how anatomical differences can cause blood flow heterogeneity, nor have any textbook in the office knowledge on lung physiology referred to this issue.

However, the realization that there is a distribution pattern of blood flow through the lungs independent of gravity may suggest some anatomical differences that could contribute to this heterogeneity, such as distribution of alveolar capillaries.

Integrating anatomical gradients might help improve the model of perfusion in describing non-uniformity of blood flow in healthy human lungs. This potentially leads to an

improved understanding of the mechanisms that can contribute to perfusion heterogeneity and the matched ventilation/perfusion in normal lungs. Thus, the following problem statement will be investigated in the remainder of this project:

How is it possible to implement anatomical gradients in the model by Mogensen et al. (2010) to obtain a correct reflection of perfusion distribution? How can this help with providing better understanding of the mechanisms that contribute to perfusion heterogeneity in healthy human lungs?

4.2 Solution strategy

The aim of this project is to implement anatomical gradients in the perfusion model by Mogensen et al. (2010) and to investigate their effect on distribution of perfusion. The model of ventilation and perfusion were integrated and implemented in MatLab (Mathworks, Natick, MA) by Mads Mogensen. The MatLab code is delivered to the author at Aalborg University, Department of Health Science and Technology. Initially, the perfusion model will be described. After that, there will be examined what factors in the perfusion model could be used to describe the perfusion heterogeneity due to anatomical gradients. Thereafter, models of anatomical gradients will be explained and implemented in the perfusion model. The report will contain a parameter analysis to investigate the influence of adjusting anatomical gradients on the perfusion distribution down the lungs. Finally, the effect of implementing anatomical gradients in the perfusion model will be studied at prone posture whereafter a discussion and a conclusion wrap up the results of the project. Therefore, the strategy for answering the problem statement is determined in the following parts:

Part II - Material Description

This part of the study will describe the perfusion model by Mogensen et al. (2010). The data sets for validation will be described, as well.

- The Perfusion Model
- The Data Sets for Validation

Part IV - Implementation and Results

This part will be dealing with implementation of the parameters that affect pulmonary perfusion. The results of implementing the anatomical gradients in the model of perfusion will be presented. Sensitivity analysis of anatomical parameters will performed to test the model behavior at different anatomical gradients. The objective is to examine how well the model can mimic the experimental data and what enhancements will be obtained by implementing the anatomical gradients of perfusion.

- Implementation
- Resuts
  - Sensitivity Analysis

Part V - Studying the Effect of Anatomical Gradient

The purpose of this part is to investigate the effect of implementation the anatomical gradients on perfusion distribution in the prone posture. This will be done to investigate the hypothesis that anatomical gradients contribute to distribution of perfusion down the lungs.

- The Effect of Anatomical Gradient at prone posture

Part VI - Synthesis

The results are discussed and summarized in the synthesis. Based on the results, a conclusion will be presented.

- Discussion
- Conclusion

Part II

Material Description

Chapter 5

The Perfusion Model

The aim of this chapter is to introduce the perfusion model that has been formulated by Mogensen et al. (2010)to the reader. The model is based on a number of assumptions and mathematical equations which together describe the distribution of pulmonary perfusion down the lungs due to the effect of gravity. The following sections will be dealing with these assumptions and the generic design of the model.

5.1 Model assumptions

- Computing the hydrostatic pressure of blood was done with reference to the pressure in the pulmonary valve, assuming it to be 5 cm down the lungs in the supine position.
- The density of blood and tissue in the lungs were assumed constant.
- Tissue and blood in the large vessels were assumed to be distribute equally between lung layers.
- It was assumed that the capillary transmural pressure determines the cross-sectional shape of the capillary.
- The flow of blood was assumed laminar with Newtonian properties.
- Constant capillary circumference at negative capillary transmural pressure.
- The number of capillaries per alveolus is assumed to be constant, thus it was constant for all lung layers because each layer was assumed to contain the same number of alveoli, see appendix A.1.2.
- The blood pressure in the pulmonary vein was assumed to be constant during systole and diastole.

- The pulmonary alveolar capillaries were assumed to be arranged in the same manner.
- Air density is negligible.

5.2 Model description

The lungs are modeled as stratified, each layer reflects a vertical height. Figure 5.1 is a schematic illustration showing a computer tomographic image of the lungs as they are divided into 10 horizontal layers (i=1:10) for the sake of simplicity. A schematic representation of the capillary and alveolar model is shown, as well.

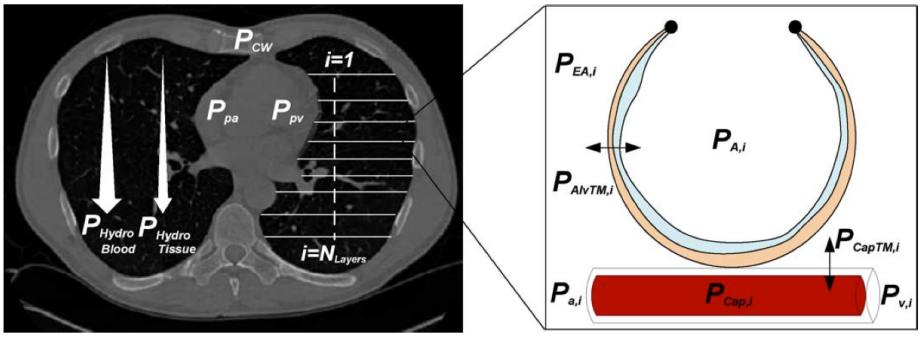

Figure 5.1: *Schematic Illustration of of the perfusion model. Left, a computed tomographic image of the transverse plan for a subject in the supine position shows the lungs as divided into 10 horizontal planes. The layer index (i) controls the layer depth which increments downwards.* $P_{HydroBlood}$ *and* $P_{HydroTissue}$ *are hydrostatic pressures exerted by lung tissue and blood, respectively;* P_{CW}*: chest wall pressure. Right, a schematic representation of the alveolar model.* $P_{\mathrm{EA},i}$*: extraalveolar pressure;* P_{A}*: airway pressure;* $P_{AlvTM,i}$*: alveolar transmural pressure;* $P_{A,i}$*: alveolar pressure;* $P_{CapTM,i}$*: capillary transmural pressure;* $P_{a,i}$*: artery pressure:* $P_{v,i}$*: venous pressure. [Mogensen* et al.*, 2010]*

The model includes the effect of lung height on perfusion, from non-dependent to dependent layer, due to the lung tissue weight on the layers below which results in a hydrostatic gradient ($P_{HydroTissue}$). In addition, the blood in the capillary network causes a hydrostatic gradient ($P_{HydroBlood}$) increasing blood pressure down the lungs.

Equations 5.1 and 5.2 were used to calculate the hydrostatic pressure due to lung tissue and blood, respectively.

$$P_{HydroTissue} = \sum_{j=1}^{i} \rho_{Lung} \cdot g \cdot t_j \tag{5.1}$$

$$P_{HydroBlood} = \sum_{j=1}^{i} \rho_{Blood} \cdot g \cdot (t_j - D_0) \tag{5.2}$$

Where ρ_{Lung} and ρ_{Blood} are the density of lung (tissue and blood) and blood, respectively. t_j is the thickness from layer $j = 1$, and g is the gravitational acceleration. The hydrostatic blood pressure was calculated with reference to the pressure in the pulmonary valve at position D_0. The density of the lung in layer i were calculated using equation 5.3.

$$\rho_{Lung,i} = \frac{\rho_{Tissue} \cdot V_{TissuePrLayer} + \rho_{Blood} \cdot (V_{CapBlood,i} + V_{VesselBloodPrLayer})}{V_{TissuePrLayer} + V_{CapBlood,i} + V_{VesselBloodPrLayer} + V_{Air,i}} \tag{5.3}$$

Where $V_{Air,i}$ is the volume of air, and $V_{CapBlood,i}$ is the volume of capillary blood, both for layer i. $V_{VesselBloodPrLayer}$ and $V_{TissuePrLayer}$ are the volume of tissue per layer and the volume of blood per layer are calculated using equation 5.4 and 5.5, respectively.

$$V_{TissuePrLayer} = \frac{V_{Tissue}}{N_{Layers}} \tag{5.4}$$

$$V_{VesselBloodPrLayer} = \frac{V_{VesselBlood}}{N_{Layers}} \tag{5.5}$$

Where N_{Layers} is the number of layers the lungs are divided into, whereas V_{Tissue} and $V_{VesselBlood}$ are the total volume of tissue and blood in the lungs.

The extraalveolar pressure, P_{EA} influences both alveolar and capillary transmural pressure, which is how the airway and capillary pressures are coupled in the perfusion and ventilation models. P_{EA} was defined as shown in equation 5.6.

$$P_{EA,i} = P_{CW} + P_{HydroTissue} \tag{5.6}$$

Where P_{CW} is the chest wall pressure which was stated in the ventilation model in equation.

The number of alveoli and capillaries in each layer were modeled to be constant regardless of layer depth. However, only one capillary per alveolus is shown in Figure 5.1 for the sake of simplicity. The number of capillaries in each layer, $N_{CapPrLayer}$, was calculated by equation 5.7.

$$N_{CapPrLayer} = \frac{N_A}{N_{Layers}} \cdot N_{CapPrAlv} \tag{5.7}$$

Where N_A is the total number of alveoli in the lungs, which was estimated by [Angus and Thurbeck, 1972] to be 375 million. The number of capillaries surrounding each alveolus, $N_{CapPrAlv}$, was modeled as a constant for each layer from ventral to dorsal

part of the lungs. Determination of blood perfusion, $Q_{Cap,i}$, through a capillary in a layer can be done by equation 5.8.

$$Q_{Cap,i} = \frac{P_{a,i} - P_{v,i}}{R_{Cap,i}} \tag{5.8}$$

Where $P_{a,i}$ and $P_{v,i}$ are the artery and venous pressure that were computed using equations 5.9 and 5.10, respectively.

$$P_{a,i} = P_{pa,i} + P_{HydroBlood,i} \tag{5.9}$$

$$P_{v,i} = P_{pv,i} + P_{HydroBlood,i} \tag{5.10}$$

Where $P_{pa,i}$ is the pulmonary artery pressure at the level of the pulmonary valve assuming to lie 5 cm down the lungs. $P_{pv,i}$ is the pulmonary venous pressure at the level of pulmonary venous valve. $P_{pv,i}$ was assumed to be constant during systole and diastole, but only changes due to increased hydrostatic pressure down the lungs.

In each lung layer, the capillary transmural pressure, $P_{CapTM,\,i}$, was computed using equation 5.11

$$P_{CapTM.i} = P_{Cap,\,i} - P_{EA.i} \tag{5.11}$$

However, the capillary transmural pressure is not homogenous along the entire capillary length. The capillary pressure should decline along the capillary from arteriole to vein. Therefore, the alveolar capillary was designed as divided into number of segments, as illustrated in Figure 5.2. The pressure inside the first capillary segment, $P_{Cap,i,1}$, was assumed to be equal to pulmonary artery pressure, whereas the pressure of the last capillary segment,$P_{Cap,i,4}$, was assumed to be equal to the pulmonary venous pressure.

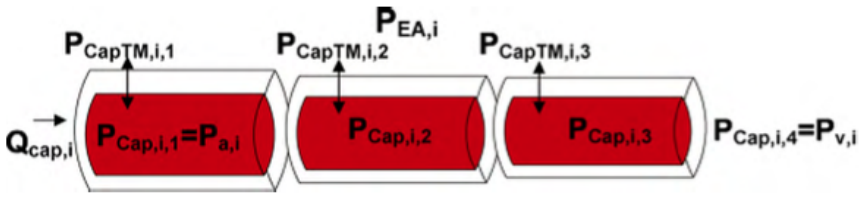

Figure 5.2: *Illustration of the capillary model showing the capillary divided into three segments. Each segment in layer i has a pressure drop due to capillary decreased radius. $P_{EA,i}$, extraalveolar pressure. $P_{a,i}$, arterial pressure in layer i. $P_{v,i}$, venous pressure in layer i. $P_{CapTM,i}$, capillary transmural pressure in layer i. $P_{Cap,i,n}$, capillary pressure at segment n. $Q_{Cap,i}$ is the capillary flow in layer i. [Mogensen* et al.*, 2010]*

The problem of identifying pressure drop in each segment can be solved using equation 5.12. It is known that the blood flow in each segment of the capillary is the same. This

yields n equations with n unknowns, the $Q_{Cap,i}$ and $P_{Cap,i,[2,...n]}$. That is, if there is three capillary segment, then the unknowns will be $Q_{Cap,i}$, $P_{Cap,i,2}$, and $P_{Cap,i,3}$.

$$Q_{Cap,i} = \frac{P_{a,i} - P_{v,i}}{R_{Cap,i}} = \frac{P_{Cap,i,n} - P_{Cap,i,n+1}}{R_{Cap,i,n}}; n = [1 : N_{Segments}] \tag{5.12}$$

The capillary cross-section was modeled to have a circular shape at positive transmural pressure, but becomes elliptic at negative transmural pressure. Thus, the cross-sectional shape of the capillary can be described by two radii, $r_{1,i,n}$, $r_{2,i,n}$, for each segment. Changes in capillary $r_{2,i,n}$ was modeled as a function of P_{CapTM}, as shown in equation 5.13. r_1 is determined using equation 5.14 at negative transmural pressure.

$$r_{2,i,n} = 1\mu m + \frac{5.5\mu m}{1 + e^{-(P_{CapTM,i,n} - 2.11kPa/0.8401kPa)}} \tag{5.13}$$

$$o_{i,n} = \pi \cdot (3 \cdot (r_{1,i,n} + r_{2,i,n}) - \sqrt{(r_{1,i,n} + \cdot r_{2,i,n}) \cdot (3 \cdot r_{1,i,n} + r_{2,i,n})} \tag{5.14}$$

Where $o_{i,n}$ is the circumference at negative transmural pressure. Based on that, the capillary resistance can be determined using a modified Poiseuille's low, as stated in equation 5.15.

$$R_{Cap,i,n} = \frac{0.75 \cdot L_{Cap} \cdot \eta_{Blood}(r_{2,i,n})}{r_{1,i,n} \cdot (2.r_{2,i,n})^3 \cdot M_0} \tag{5.15}$$

Where L_{Cap} is the length of capillary segment, η_{Blood}, the blood viscosity, was modeled as a function of the smallest radius when the capillary cross-section becomes elliptic. M_0 is a correction factor stated as a function of $r_{2,i,n}/r_{1,i,n}$ ratio.

The total capillary blood flow in the complete pulmonary system was computed applying equation 5.16

$$Q = \sum_{i=1}^{N_{Layers}} Q_{Cap,i} \cdot N_{CapPrLayer} \tag{5.16}$$

The capillary blood volume , $V_{Cap,i}$ can be calculated by summing up blood volume for all capillary segments, as stated in equation 5.17

$$V_{cap,i} = \sum_{i=1}^{N_{Layers}} \frac{\pi}{N_{Segment}} \cdot L_{Cap} \cdot r_{1,i,n} \cdot r_{2,i,n} \tag{5.17}$$

Where L_{Cap} is the length of a capillary segment.

5.2.1 Lung profile during breathing

A lung profile was constructed using high resolution CT-scans of a heathy human at total lung capacity. A profile of cross-sectional area for the frontal plane as a function of depth, D, is shown in Figure 5.3A. The CT-scans were 394 slices each of which had a resolution of 512×512 pixels and separated by 1 mm thickness from the lung apex to the base. The profile was constructed to be used in model simulation of supine posture. The number of pixels at a given depth were summed up for all scans from the lung ventral part, multiplying by the pixel dimension 0.7813mm×1mm.

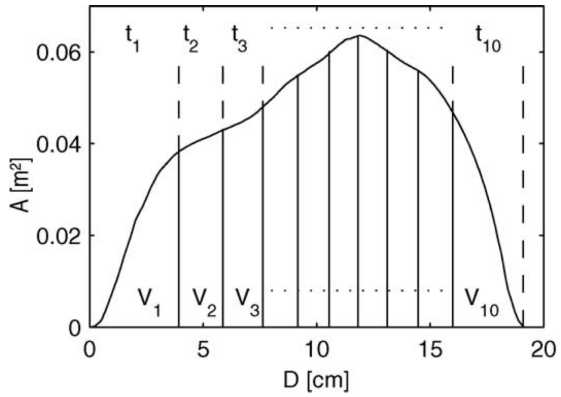

Figure 5.3: *A: a profile of the lungs of a subject in the supine position showing the relationship between the cross-sectional area, A, and lung depth, D, at total lung capacity (solid line). The profile of the lungs is divided into 10 layers for the sake of simplification. t_i, the thickness, and V_i, the volume, of layer i are presented. The figure is modified from [Steimle* et al.*, 2010]*

5.2.2 Model parameters

Simulation of the perfusion model is dependent on a number of parameters. Table 5.1 presents these parameters and their values.

Parameter	Value	Description
N_{Layer}	100	Number of layers
$N_{CapPrAlv}$	15	Number of capillaries per alveolus
N_A	375 mio	Number of alveoli
L_{Cap}	350 μm	Length of capillary

Table 5.1: Parameters of the perfusion model. A Part of the table content is adopted from [Mogensen et al., 2010]

5.3 Arteriole resistance

Because pulmonary arterioles are smaller in radius than arteries, it is important to consider the arteriole resistance when computing blood flow from the pulmonary artery to vein. That is, the resistance to blood flow will be a combination of the pulmonary arteriole resistance and capillary resistance. This motivated Mogensen and his colleagues to implement this effect in the model of perfusion, which showed an enhancement in simulation of the pulmonary perfusion. Thus, equations 5.8, 5.9, and 5.12 were updated to include the effect of arteriolar resistance ($R_{Art,i}$) and pressure ($P_{Art,i}$). The equations based on an unpublished article.

$$Q_{Cap,i} = \frac{P_{Art,i} - P_{v,i}}{R_{Art} + R_{Cap,i}} \tag{5.18}$$

$$P_{Art,i} = P_{pa,i} + P_{HydroBlood,i} \tag{5.19}$$

$$Q_{Cap,i} = \frac{P_{Art,i} - P_{v,i}}{R_{Art} + R_{Cap,i}} = \frac{P_{Cap,i,n} - P_{Cap,i,n+1}}{R_{Cap,i,n}}; n = [1 : N_{Segments}] \tag{5.20}$$

Figure 5.4A and 5.4B shows the capillary model where arteriole pressure is added, which is calculated by equation 5.19 at the different lung layers. The arteriolar resistance was assumed constant at the different lung layers.

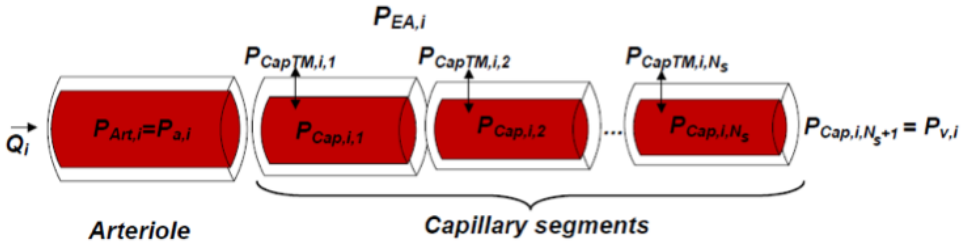

Figure 5.4: *Schematic Illustration of the capillary model showing the capillary divided into N_S segments. Each segment in layer i was modeled to have a pressure drop due to decreased capillary radius. P_{EA}, extraalveolar pressure. $P_{Art,i}$, arteriole pressure. $P_{a,i}$, arterial pressure. $P_{v,i}$, venous pressure. $P_{CapTM,i}$, capillary transmural pressure. P_{Cap,i,N_S}, capillary pressure at segment N_S. Q_i is the capillary flow. [Steimle* et al.*, 2010]*

Simulation results before and after incorporating the arteriolar resistance are shown in Figure 5.7A and 5.7B, respectively. Figure 5.7A is reprinted for the sake of comparison. In both figures, pulmonary perfusion is calculated relative to mean down the lungs. The model parameters used in the both cases are: N_{Cap}=15; $N_{Segment}$=20; N_{Layer}=100; L_{Cap}=350 μ m; and 12 breaths. R_{Art} is set to be 0.5 kPa s/nl.

Figure 5.7B will be used in the following chapter when comparison between simulations before and after including an anatomical gradient is performed.

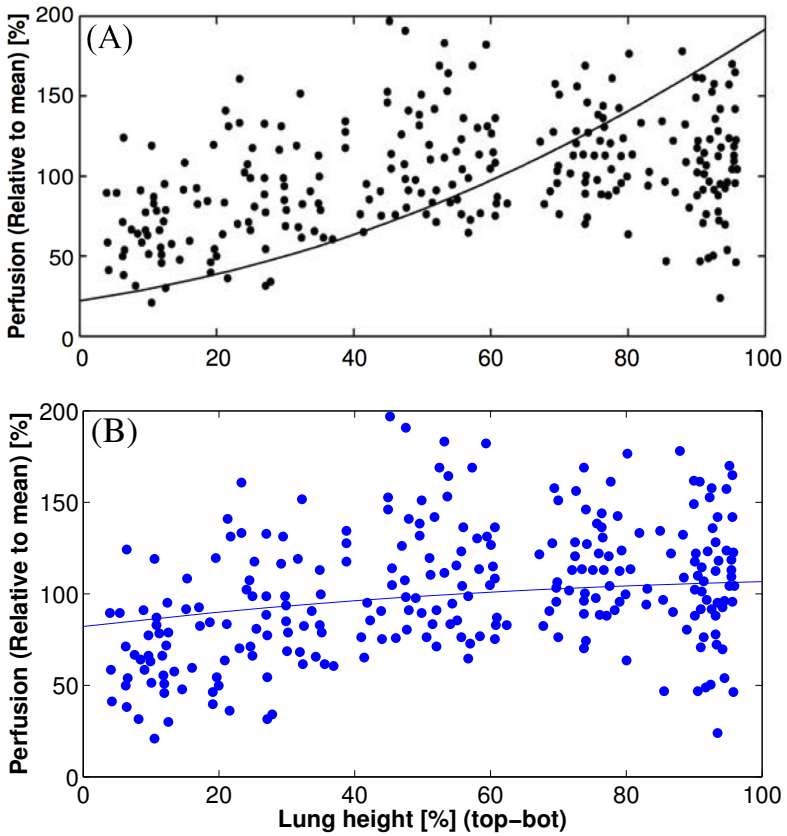

Figure 5.5: *A: perfusion distribution down the lungs without arteriole resistance (R_{Art}= 0.5 kPa s/nl). B: Simulation results of the perfusion model when including the effect of constant arteriole resistance at the different lung layers. The simulation was performed using the same parameters: N_{Cap}=15; $N_{Segment}$=20; N_{Layer}=100*; L_{cap}= 350 μ m; and 12 breaths

5.4 The model default values

A number of values in the perfusion model were set as default. These values were specified by Mogensen et al. as shown in table 5.2.

Parameter	Default value	Description	Reference
D_0	5 cm	Depth of pulmonary valve down the lungs in supine position	[Ferner and Staubesand, 1982]
ρ_{Blood}	1.060 g/cm^3	Density of blood	[Kenner, 1989]
ρ_{Tissue}	1.0 g/cm^3	Density of lung tissue	[A.B. Millar, 1989]
V_{Tissue}	450 ml	Volume of lung tissue	[Steimle et al., 2010]
$V_{VesselBlood}$	377 ml	Volume of blood in large vessels	[Lewis et al., 1970]
g	9.81 m/s^2	Gravitational acceleration	[Angus and Thurbeck, 1972]
P_{pv}	1.066 kPa	Pulmonary venous pressure at the level of the pulmonary valve	[Lambert et al., 1982]
$N_{Segments}$	20	Number of capillary segments	[Mogensen et al., 2010]
O	8.88 μm	Capillary circumference at negative transmural pressure	[Mogensen et al., 2010]
$Resolution$	200	Number of pressure steps in a breath	[Mogensen et al., 2010]
R_{Art}	0.5 kPa s/nl	Arteriolar resistance	[Mogensen et al., 2010]
$N_{Breaths}$	12	Number of breaths	[Mogensen et al., 2010]

Table 5.2: The default values of the perfusion model. A Part of the table content is adopted from [Mogensen et al., 2010]

5.5 Solving the perfusion model

An optimization algorithms are applied to solve the model basing on the Newton-Rapson method for finding solutions in each iteration in the model. Inside the ventilation model, the perfusion model is solved in two levels. In each level, an optimization algorithms is used.

5.5.1 The first level

The first level is simplified in Figure 5.6 using a pseudocode. The algorithms are divided into two parts, the first iteration and the remainder iterations.

In the first iteration of this level, an initial guess of lung volume and blood flow is made. Using the guessed lung volume, a value of chest wall pressure,P_{CW}, is calculated by calling equation A.2, see appendix A. Thereafter, the algorithms will compute the following for each lung layer: the extra-alveolar pressure P_{EA} from P_{CW} and $P_{HydroTissue,i}$ from equation 5.6 and equation 5.1, respectively; the artery pressure from equation 5.9 using the hydrostatic pressure of blood, $P_{HydroBlood,i}$, from equation 5.2; calling the second level of the algorithm for calculating the capillary blood flow using the initial guess of blood flow as well as the above calculated values as an input; computing the capillary volume by calling `getCapVolume` with capillary radii as an input; the capillary blood volume in layer i; and the volume of the alveolus in layer i. By summing up the volume of each layer added to that the anatomical dead space, the difference (`Delta`) between the calculated and guessed lung volume can be determined. Finally, the program provides a new guess for the lung volume.

In the remainder iterations, a `WHILE` loop is provided for controlling the program. The algorithm start again with calculating the chest wall pressure with input from the new guessed volume to be used in each calculation of lung layers inside `FOR` loop. The `WHILE` loop ends with computing (`Delta`) as well as a new guess for the lung volume.

First iteration:

```
1 Initial GuessVLung
2 Initial GuessFlow
3 CALL Pcw(GuessVolume)
4 RETURN Pcw
5  FOR each Layer of the lungs from i=1:NLayer
6     COMPUTE PEA,i from Pcw and PHydroTissue,i
7     COMPUTE Pa,i from Ppa and PHydroBlood,i

8       CALL getCapillaryFlow(GuessFlow,PEA,i,Pa,i,PHydroTissue,i)
9       RETURN QCap,i

12    CALL getCapVolume(CapRadius1, CapRadius2)
13    RETURN VCap,i
      COMPUTE VBloodInLayer,i from VCap,i
      COMPUTE volume of the alveolus, VA
14  END FOR
15 COMPUTE Total lung volume from VA + anatomical deadspace

16 COMPUTE Delta between GuessVLung and Total volume
17 COMPUTE NewGuessVolume
```

The remainder iterations:

```
1 WHILE Delta > Tolerance intervel
2   CALL Pcw(NewGuessVolume)
4   RETURN Pcw
3     FOR each Layer of the lungs from i=1:NLayer
4         Do the same as above inside the FOR LOOP
5     END FOR
6   COMPUTE Total lung volume
7   COMPUTE Delta between Guess and Total volume
8   COMPUTE NewGuessVolume
9 END WHILE
```

Figure 5.6: *A pseudocode describing part of the model code. The first level of solving the perfusion model is contained in the ventilation model. The second level of the perfusion model is called by* `getCapillaryFlow()`

5.5.2 The second level

The second level of the algorithms is divided into two parts, the first iteration and the remainder iterations:

In the first iteration, the capillary pressure in each segments is calculated. Initially, the pressure drop $P_{DeltaArt}$ cross the arteriole is computed using equation 5.20 from

the value of arteriole resistance and an initial guess of blood flow. The capillary pressure inside the first segment, $P_{Cap,1}$, is computed from the artery pressure, P_a, and $P_{DeltaArt}$. The capillary transmural pressure, $P_{CapTM,1}$, is then computed from the capillary pressure using equation 5.11. Thereafter, calculations will be repeated for remainder of each capillary segments: $P_{Cap,i}$ from pressure inside the last capillary segment, $P_{Cap,i-1}$, and pressure drop across it, $P_{DeltaCap,i-1}$; capillary transmural pressure, which is then utilized to computed capillary radius $r_{2,i.n}$ by equation 5.13; computing capillary radius, $r_{1,i,n}$, using equation 5.14; computing the blood viscosity using input from $r_{1,i,n}$; calling equation 5.15 for calculating the capillary resistance with the inputs from $r_{1,i,n}$, $r_{1,i,n}$, and blood viscosity; and finally the pressure drop $P_{DeltaCap,i}$ across the capillary segment i is computed. The pressure at the capillary end, P_{CapEnd}, is determined from $P_{DeltaCap,i}$ and $P_{Cap,i-1}$.The error between P_{CapEnd} and $P_{DeltaCap,i}$ is computed to be used in next iteration.

The reminder iterations are controlled by a `WHILE` loop. Inside the `WHILE` loop the same algorithms as in the first iteration are repeated. For each iteration error is calculated and compared with a defined tolerance interval. The calculation will be repeated while computed error is higher than the tolerance interval. The final capillary flow is therefore determined from the last guess.

First Iteration:

```
1 Initial GuessFlow
2 COMPUTE PDeltaArt from RArt and GuessFlow
3 FOR each capillary Segment from i=1:NSegments
4     IF first Segment
5       COMPUTE PCap,1 = Pa - PDeltaArt
6       COMPUTE PCapTM,1 = PCap,1 - PEA,1
7     ELSE
8       COMPUTE PCap,i = PCap,i-1 - PDeltaCap,i-1
9       COMPUTE PCapTM,i = PCap,i-1 - PEA,i-1
10    END IF
11       COMPUTE CapRadius2(PCapTM,i)
12       COMPUTE CapRadius1(CapRadius_2)
13    CALL bloodViscosity(CapRadius_2(i))
14    RETURN viscosity(i)
15
16    CALL getCapResistance(Radius1,CapRadius2,viscosity)
17    RETURN RCap,i
18
19    COMPUTE PDeltaCap,i from GuessFlow and RCap,i
20 END FOR
20 COMPUTE PCapEnd = PCap,i - PDeltaCap,i
21 COMPUTE Error = PCapEnd - Pv,i
```

The remainder Iterations:

```
1 WHILE Error > Tolerance interval
2     FOR each capillary Segment from i=1:NSegments
3       Do the same as above inside FOR LOOP
          :
          :
4     END FOR
5 COMPUTE a new GuessFlow
6 COMPUTE PCapEnd = PCap,i - PDeltaCap,i
7 COMPUTE Error = PCapEnd - Pv,i

8 END WHILE
9 Final flow = last GuessFlow
```

Figure 5.7: *A pseudocode describing how the capillary model is solved.*

Chapter 6

The Data Sets for Validation

The purpose of this chapter is to describe the experimental data sets that will be used to validate the results of simulation from the perfusion model.

6.1 Experimental data from Jones et al. (2001)

Jones et al. (2001) investigated pulmonary perfusion in healthy human subjects in both supine and prone posture applying electron-beam computed tomography (CT-scanner, Imatron C150L). Six healthy subjects (23-44 years) participated in the experiment. As the subjects were placed in a CT-scanner, imaging was established on intermittent positive-pressure ventilation (breath holding) with inspired oxygen fraction of 0.21 and tidal volume of 10-12 ml/kg (mean 0.935l). The experimental data is presented as pulmonary perfusion per volume lung parenchyma (without air) and was reported as perfusion in comparison to mean perfusion. Experimental data read from Jones et al. (2001) is represented in Figure 6.1 where a curve of second order polynomial is fitted ($R^2 = 0.215$, RMSE= 31.06) presenting the general trend of the data.

The experimental data by Jones et al. (2001) showed in general an increase in pulmonary perfusion form non-dependent regions towards the dependent regions of the lungs, with high variability of pulmonary perfusion at each lung depth.

The experimental data is in agreement with other experimental data e.g. [Glenny et al., 1991, Glenny et al., 2000, Prisk et al., 1994] in that there is a blood flow reduction in the most dependent part of the lungs (zone 4). The data is used to calibrate the model, describing the perfusion distribution in the different parts of the lungs due to anatomical gradients.

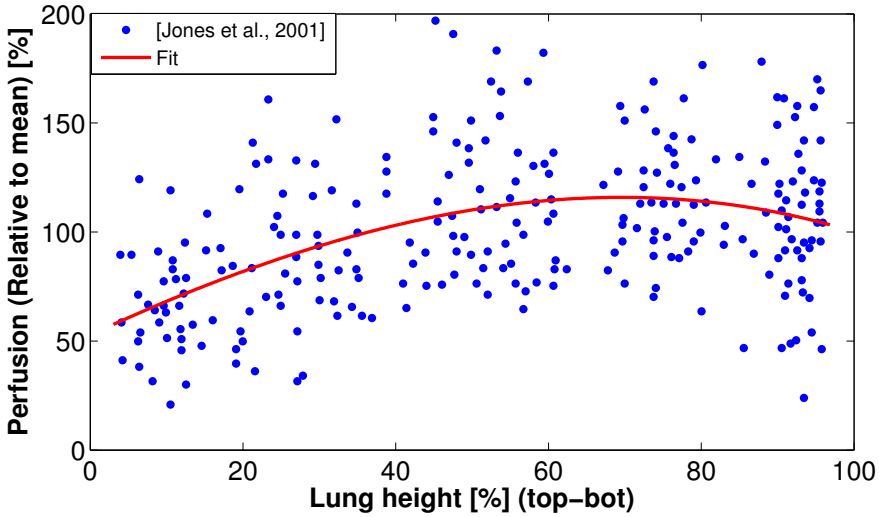

Figure 6.1: *Perfusion distribution from top(ventral part) to bottom(dorsal part) for subjects in supine posture. Dots: Experimental data read from Jones et al. (2001) for 6 healthy human subjects in the supine posture; red line: a curve of second order polynomial fitted to the experimental data (R^2=0.215) presenting the trend of the data. The measured perfusion were normalized relative to mean perfusion and was presented in percentage*

Part III

Implementation and Results

Chapter 7

Implementation

This chapter deals with implementation of the anatomical gradients in the lung model of perfusion. This will be done to investigate the effect of anatomical gradients on perfusion distribution in the lungs.

7.1 Choosing the anatomical parameters

As has been described in section 2.1, several studies, e.g. [Glenny et al., 1999, Glenny et al., 1991, Glenny and Robertson, 2011], have reported the importance of anatomical gradients in describing the heterogeneity in perfusion distribution in normal healthy lungs. These studies suggested that geometry and branching of vascular tree can have an effect on distribution of perfusion. Examining the distribution pattern down the lungs, numerous studies, e.g. [Amis et al., 1984, Hakim et al., 1987, Hakim et al., 1988, Levin et al., 2001, Glenny et al., 1999, Glenny et al., 1991, Glenny et al., 2000], showed a persistent pattern of perfusion heterogeneity, with decreasing blood flow distribution towards the lung peripheries in all directions. This perhaps indicate a number of parameters that could vary with distance from the center of the lungs. These parameters could be the geometry of alveolar capillary networks, capillary inner radius, length, elasticity, and density of capillary network. The question of what anatomical parameters that can contribute to heterogeneity of perfusion in the lungs maybe valuable to answer, which might lead to understand the mechanism of the matched ventilation/perfusion in normal lungs.

Considering how the vascular tree is bifurcated, the pattern may seems as presented in Figure 7.1, which shows asymmetric branching of the vascular tree. Bifurcations of vascular tree causes a reduction in the diameter and length of the daughter branches. The bifurcation of the daughter branches terminate at the arteriolar level, where no more branches will appear. From this terminal, the arterioles begin to bifurcate to capillaries. Mechanisms might contribute to heterogeneity of perfusion distribution could be that the alveolar capillaries become longer and the number is higher as the daughter branch is far away from the artery.

In the perfusion model, simulation of the pulmonary perfusion depends on number of parameters. The majority of these parameters are not related to the anatomy of the vascular tree. These parameters are determined by number of experiments, see table 5.2. Considering how the capillary was described in the perfusion model, two parameters are found significant to use: the number (N_{Cap}) and length (L_{Cap}) of alveolar capillaries. In the model, simulation of pulmonary perfusion depends on these parameters (see equations 5.7, 5.15, 7.5, and 5.17), where an adjustment may result in a modified simulation of blood flow distribution. This motivates a gradient model for capillary number and length.

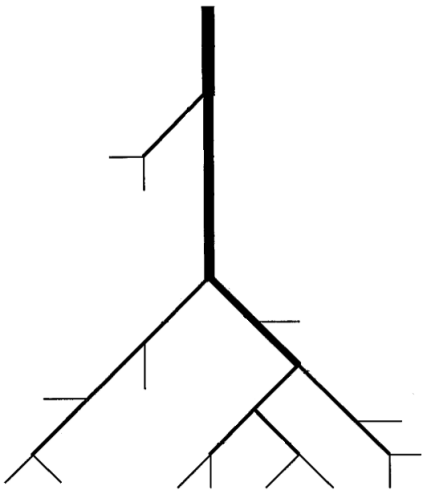

Figure 7.1: *Schematic illustration of pulmonary vascular tree. Each pulmonary vessel bifurcates into a number of vessels. The figure is modified form [Huang* et al.*, 1996]*

7.2 Implementation in the perfusion model

In order to integrate anatomical gradients in the model of perfusion, different formulae have to be modified. Because the perfusion model describes the lungs as a number of horizontal layers going from the ventral to the dorsal part of the lungs, it is convenient to utilize this effect to decide length and number of capillaries in each layer. Figure 7.2 presents a simple pseudocode describing where in the integrated models of ventilation and perfusion the gradient functions have to be implemented. Calculating perfusion and ventilation in the model occurs in two parts, in the first iteration and in the remainder iterations. In each iteration, a new guess of lung volume is made basing on the Newton-Rapson Method.

In the first iteration, an initial guess of the total lung volume is used. The algorithms compute alveolar perfusion and ventilation for each layer inside a `FOR` loop. Thus, the gradient functions (`numOfCap`: capillary number function; `capLength`: capillary length function) should be called inside this loop where capillary number and length have

to be used. Based on the guessed volume, the model calculate volume of the lungs. Thereafter, the difference between the guessed and computed lung volume is computed (`Delta`) .

In the remainder iteration of the algorithms, a `WHILE` control the iterations by comparing `Delta` with a specified tolerance interval. For the different lung layers recomputing the perfusion and ventilation is performed by a `FOR` loop. Inside the `FOR`, calling the gradient functions allows to determine the length and number of alveolar capillaries to be used in the calculation. The optimization algorithms will be repeated for each new guessed lung volume.

First iteration

```
Initial Volume Guess
FOR each layer of the lungs from top to bottom
        :
        :
       CALL numOfCap with layer number
       CALL capLength with layer number
        :
        :
       CALL perfusion function
       COMPUTE alveolar volume
END FOR
COMPUTE Total lung volume
COMPUTE Delta between Guess and Total volume
COMPUTE NewGuessVolume
```

The rest iterations

```
WHILE Delta > Tolerance interval
  FOR each layer of the lungs from top to bottom
            :
            :
           CALL numOfCap with layer number
           CALL capLength with layer number
            :
            :
           CALL perfusion function
           COMPUTE alveolar volume
  END FOR
  COMPUTE Total lung volume
  COMPUTE Delta between Guess and Total volume
  COMPUTE NewGuessVolume
END WHILE
```

Figure 7.2: *A part of the model code is simplified by using pseudocode to illustrate where in the model the gradient functions have to be implemented.* ***numOfCap****, the function of capillary number gradient.* ***capLength****, the function of the capillary length gradient.*

7.3 Gradient functions

In order to describe the gradient of perfusion down the lung, the MatLab membership functions `pimf()` and `trimf()` are chosen. The functions provide flexible curves by adjusting the functions' input parameters. The gradient function `pimf()` is defined as follows:

$$Intensity = pimf(\ layerNum, [\ a\ b\ c\ d\ ]\ ) \tag{7.1}$$

Where `Intensity` is the output of the function for the input *layerNum*, which is the layer index. The function's input parameters specify a 4-elements vector, where "a" and "d" determine the "feet" of the curve, while "b" and "c" determine the function's center. The function is evaluated at each calculation of perfusion through the lung's different layers. Thus, the input to this function is the lungs' layer number (layerNum) from ventral (top) to dorsal part (bottom) of the lungs. The function's output describes the degree of membership (intensity) of the input elements, assigning a value to it between 0 and 1. Figure 7.3 is a plot illustrating two examples using the function described above. The slope of the curve can be used to describe intensity gradient for each index of input layer. The number of the layers in the figure is specified to be 20 for simplicity. The curve with the solid line illustrates output of the input parameters: a=-9; b=10; c=10; d=31. Whereas the curve with broken line represents output of the same function where input parameters are: a=-19; b=15; c=15; d=41. Note that the center of the curve is moved from layer 10 to layer 15 down the lungs, while the slope gradient become smaller towards the lungs' peripheries.

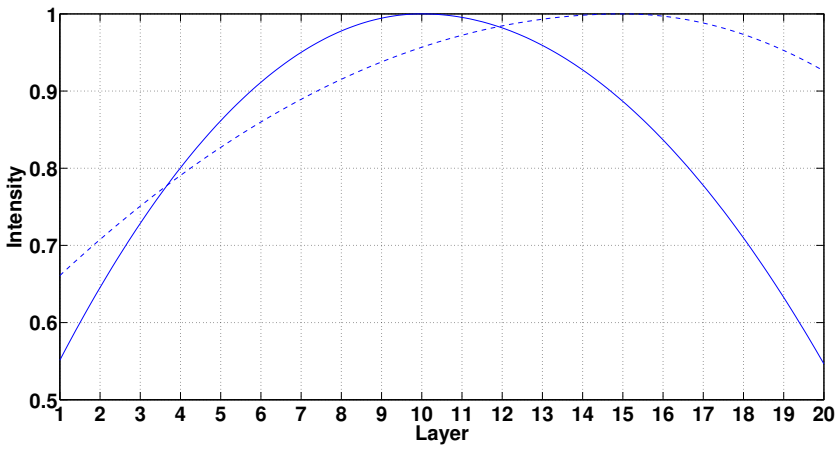

Figure 7.3: *A Plot of the MatLap function* `pimf(layerNum,[a b c d])` *demonstrating two examples of input for parameter vectors: solid line, parameters=[-9 10 10 31]; broken line, parameters=[-19 15 15 41]*

The function `trimf()` is applied to create a linear gradient. The function is defined as:

$$Intensity = trimf(\ layerNum, [\ e\ f\ g\ ]\ ) \tag{7.2}$$

Where [e f g] is the input vector, "e" and "g" are the "feet" of the curve while "f" is the center of the curve. Figure 7.4 is a plot of the function using two different vectors: a symmetric vector [-9 10 31]; and non symmetric vector [-19 15 41].

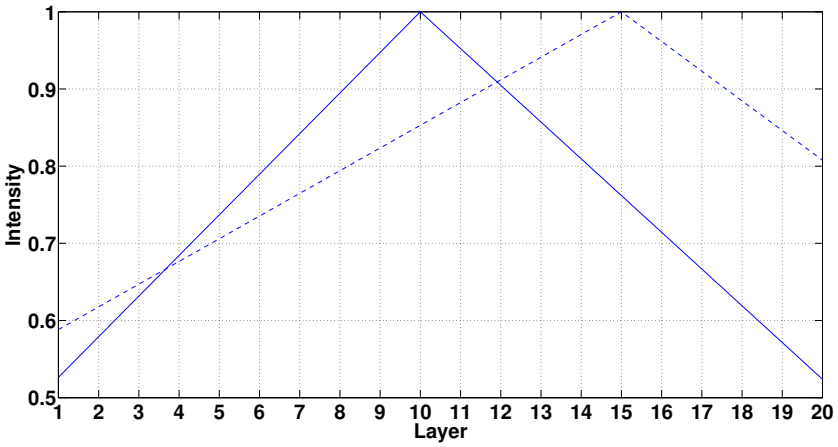

Figure 7.4: *A Plot of the MatLap function* `trimf(layerNum,[a b c d])` *demonstrating two examples of input for parameter vectors: solid line, parameters=[-9 10 31]; broken line, parameters=[-19 15 41]*

In order to simulate the pulmonary heterogeneous distribution of perfusion some assumptions have to be carried out. the following section will list these assumptions.

7.4 Assumptions

Based on the studies explained in chapter 2 which showed a pattern of perfusion heterogeneity down the lungs, a number of assumptions are made in order to mimic the distribution of perfusion:

- It is assumed that the number of capillaries suppling the alveolus defers from the top to the base of the lungs due to the difference in number and length of pulmonary capillaries surrounding the alveoli.
- There is a gradient describing the length of the alveolar capillary from the top to the base of the lungs.
- All alveolar capillaries have the same elastic properties.

In order to describe the distribution of perfusion due to anatomical gradients, different equations of the perfusion model have to be altered. The following section will deal with these equations.

7.5 Equations

A number of equations of the perfusion model are adjusted in a way that they can receive the number of capillaries or the capillary length in each calculation. These equations are described below with their belonging gradient function.

7.5.1 Gradient of capillary number

When a gradient function is called with an input from a layer index, it will return an intensity of membership, which can be used to compute the number of capillaries per alveolus in layer i ($N_{CapPrLayer,i}$), as seen in equation 7.3.

$$N_{CapPrAlv,i} = Intensity(i) \cdot N_{CapMax} \tag{7.3}$$

Where N_{CapMax} is the maximum number of capillaries per alveolus. The number of capillaries in each layer can be determined using equation 7.4.

$$L_{CapPrLayer,i} = N_{CapPrAlv,i} \cdot \frac{N_{Alv}}{N_{Layers}} \tag{7.4}$$

The total pulmonary perfusion calculated by equation 7.5 summing up perfusions of each layer.

$$Q_{Total} = \sum_{i=1}^{N_{Layers}} Q_{Cap,i} \cdot N_{CapPrLayer,i} \tag{7.5}$$

Where $N_{CapPrLayer,i}$ is the number of capillaries in layer i.

To summarize, implementing the gradient of the number of capillaries results in finding a new parameter, which is the maximum number of capillaries N_{CapMax}. This parameter has an influence on the final number of capillaries per alveolus when applying different gradients.

7.5.2 Gradient of capillary length

The same gradient functions are applied to compute the capillary length in layer i, as shown in equation 7.6.

$$L_{CapPrAlv,i} = Intensity(i) \cdot L_{CapMax} \tag{7.6}$$

Where L_{CapMax} is the maximum length the alveolar capillary. The capillary length has an effect on calculating the capillary volume,$V_{cap,i}$, as stated in equation 7.7.

$$V_{cap,i} = \sum_{j=1}^{N_{Segments}} \frac{\pi}{N_{Segment}} \cdot L_{Cap,i} \cdot r_{1,j,i} \cdot r_{2,j,i} \ ; \ i = [1 : N_{Layer}] \tag{7.7}$$

Where $L_{cap,i}$ is the length of capillary in layer i, $r_{1,j,i}$ and $r_{1,j,i}$ are capillary radii of segment j in layer i, and $N_{Segments}$ is the number of capillary segments. The volume of blood in Layer i ($V_{BloodInLayer,i}$) is, thus, calculated by equation 7.8.

$$V_{BloodInLayer,i} = V_{Cap,i} \cdot N_{CapPrAlv,i} \cdot \frac{N_A}{N_{Layers}} \tag{7.8}$$

Changes in capillary length in the different lung layers have an influence on calculating the capillary resistance in each segment of the capillary as shown in equation 7.9.

$$R_{Segment,j} = \frac{0.75 \cdot L_{Segment,i} \cdot \eta_{Blood}(r_{2,j,i})}{r_{1,j,i} \cdot (2.r_{2,j,i})^3 \cdot M_0} \tag{7.9}$$

Where $L_{Segment,i}$ is the length of a capillary segment in layer i, which is calculated by equation 7.10.

$$L_{Segment,i} = \frac{L_{Cap,i}}{N_{Segments}} \tag{7.10}$$

As a summary, applying gradient function to decide the length of capillaries in each layer leads to find a new parameter, namely N_{CapMax}. This gradient determines the final length of the capillaries in each layer at different gradient functions.

7.6 Simulation of the experimental data

In order to mimic the experimental data by Jones et al. (2001) from a subject holding a tidal volume of 0.935l, a constant alveolar pressure (P_A) at 0.9 kPa is used in the perfusion model. Computing the mean of perfusion through a capillary in the lung layer i,$Q_{MeanPrCap,i}$, is conducted using equation 7.11.

$$Q_{MeanPrCap,i} = \frac{\sum_{j=1}^{Resolution} Q_{Cap,i}(P_A(j))}{Resolution} \tag{7.11}$$

Where *Resolution* is defined as the number of steps in a breath, $Q_{Cap,i}$ is determined by equation 5.20 in section 5.2. The mean of perfusion,$Q_{Mean,i}$, in layer i is thus calculated by equation 7.12.

$$Q_{Mean,i} = Q_{MeanPrCap,i} \cdot N_{CapPrLayer,i} \tag{7.12}$$

From the means of perfusion in lung different layers, the mean blood flow through the entire lungs can be computed using equation 7.13.

$$Q_{MeanInLungs} = \frac{\sum_{i=1}^{N_{Layer}} Q_{Mean,i}}{N_{Layer}} \tag{7.13}$$

The experimental data by Jones et al. (2001) were presented as lung perfusions relative to mean in percentage. To simulate the data, equation 7.14 is used.

$$Q_{relativeToMean,i} = \frac{Q_{Mean,i}}{Q_{MeanInLungs}} \cdot 100 \tag{7.14}$$

The mean of each layer depth over a breath, $H_{Mean,i}$, can be computed using equation 7.15. The argument to the layer depth is the alveolar pressure, P_A, which is a function of discrete time step j.

$$H_{Mean,i} = \frac{\sum_{j=1}^{Resolution} H_i(P_A(j))}{Resolution} \tag{7.15}$$

Furthermore, the mean heights are normalized, dividing each one by the total lung height. The resultant layer heights are computed in percentage of lung height, as given in equation 7.16.

$$H_{Mean,i} = \frac{H_{Mean,i}}{h_{Lung}} \cdot 100 \tag{7.16}$$

Where $H_{Mean,i}$ is the height of layer i, whereas h_{Lung} is the height of the lung from ventral (top) to dorsal (bottom) in supine position.

Chapter 8

Results

This chapter deals with the results of implementing the gradient functions in the total model of the lungs. These gradients describe changes in the length and number of pulmonary capillaries surrounding the alveoli. Before a final result of this implementation is presented, a sensitivity analysis will be performed to investigate what effects the new model parameters and gradient functions will have on the model simulation of pulmonary perfusion. The aim is to find a reasonable fit to the experimental data by Jones et al. (2001) that could be used for further investigation in the next chapter.

8.1 Sensitivity analysis

Investigating the influence of the model parameters on the model's behavior can be performed by varying one parameter while holding the other parameters constant. This technique allows an examination of the response of the perfusion model to changes in only one parameter. The sensitivity analysis uses the model default values that are specified in table 5.2. However, the number of steps in a breath and number of layers are minimized to 30 and 20, respectively. Higher values of these default parameters are evaluated to have a negligible effect on simulation of perfusion. This done by comparing simulations results at low and high values of these parameters. Using low values minimize the time needed for each simulation.

The three types of alveolar capillaries (section 3.1.1) are modeled by Mogensen et al. (2010) as an approximation with one capillary model representing all three types, which makes it difficult to predict number and length of capillaries. Mogensen et al. (2010) estimated the length and number of capillaries per alveolus to be 350 μm and 15 capillaries, respectively. This was done by adjusting these parameter values manually to obtain a cardiac output, among others, that lies within a physiological interval of 5-6l/m [Despopoulos and Silbernagl, 2003] for a resting men in supine position.

However, the reference value for cardiac output depends on the studied group. For example, the mean cardiac output in resting men in supine was reported to range

between 6.0 l/min (SD: ±,age: 61-83) and 7.1 l/min (SD:±1.8, age: 24-36), whereas in woman was 5.9±1 l/min [Letner, 2005].

Adjusting the length and number of capillaries would change the value of cardiac output. Thus, varying these parameters has to be in a range that yields a cardiac output within the lower and upper interval of this reference values.

Initially, the sensitivity analysis will be performed by holding the maximum length and the maximum number of capillaries constant as been specified in table 8.1. Subsequently, the effect of changing these parameter values on simulation of perfusion will be investigated.

Parameter	Value	Description
L_{CapMax}	350 μm	The maximum length of alveolar capillary
N_{CapMax}	15	The maximum number of capillaries per alveolus

Table 8.1: The values of the new parameters and their description. The values are constant across all layers

The sensitivity analysis is divided into two part:

- Testing the model response to linear gradients in the length and number of capillaries from ventral to dorsal part of the lungs. This test enables evaluation of the sensitivity of the model to changes in the gradient of capillary number and length. The test will be performed using the gradient function `trimf()`.
- Testing the model response to curved gradients in capillary length and number, decreasing at the lung peripheries. Thus, the test will use the gradient function `trimf()`. The aim of this test is to find a reasonable fit to the experimental data by Jones et al. (2010) .The best results will be used in the next chapter to investigate the effect of anatomical gradient in different postures.

8.1.1 Linear gradients

The effect of a linear gradient is examined using the gradient function `trimf()` with gradient vector chosen to be [a 20 20] at a=-30, a=-60, and a=-200. This gradient function will be used to describe both gradient of capillary length and number. Figure 8.1 is a plot of a gradient function with the specified vectors of the function `trimf()`.

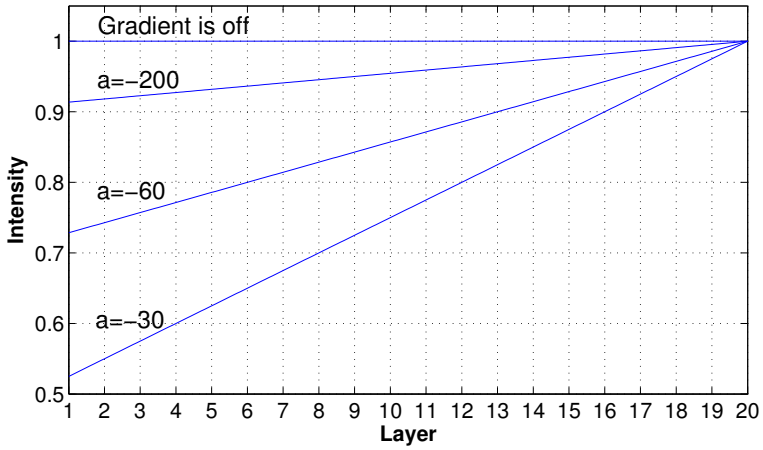

Figure 8.1: *The gradient function* `trimf()` *of the vector : [a 20 20]* where *a* parameter is specified to be - 30,-60, and -200.

The effect of implementing this gradient is shown in Figure 8.2 and Figure 8.3 for capillary number and length, respectively. In Figure 8.2A and Figure 8.2B the result of applying the gradient vector is presented. Decreasing the vector parameter *a* from -30 to -200 results in an increasing in the number of capillaries and thus perfusion at the ventral part of the lungs, while an opposite effect is presented at the dorsal part. The results show an increase in the cardiac output from 5.7 (a=-30) to 7.0 (no gradient) as the number of capillaries surrounding the alveolus are increased down the lungs.

A fixed point on the curve is presented at lung depth of 67%, independent of the style of the gradient, where all curves intersect each other. This point can be interpreted as a balance point of the curve. That is, if perfusion is reduced at the ventral part of the lungs, it will increases behind this point of the curve down the lungs; the perfusion is constant at this point.

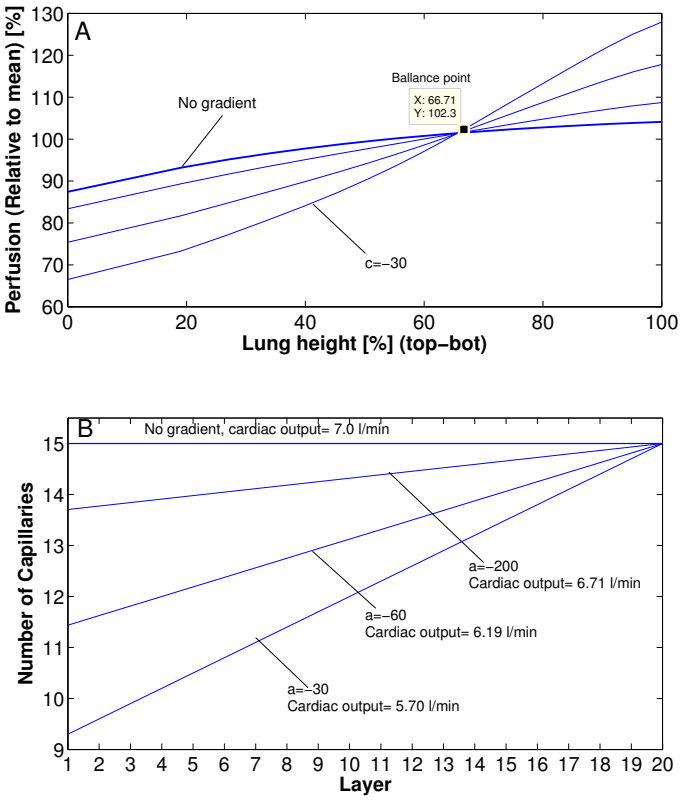

Figure 8.2: *A: simulation results of distribution of perfusion when applying linear increasing gradients by the gradient function* ***trimf()****. B: the capillary length gradient is determined using the gradient vector: [a 20 20], where a=-30, a=-60, a=-200.*

The same effect is presented when applying the gradient of capillary length, see Figure 8.3A and Figure 8.3B. However, increasing the length of alveolar capillaries has an opposite effect on the value of cardiac output than the gradient of capillary number. The influence of changing function parameter a leads to slightly decrease in cardiac output from 7.13 (a=-30) to 7.0 (no gradient). Figure 8.3A shows simulations of perfusion distribution for the respective gradient vectors. Gradient of capillary number from a=-30 to no gradient causes reduction in blood flow distribution in the non-dependent regions and an increase in the dependent regions of the lungs. Additionally, the balance point is moved slightly from lung depths of 67% to 59% towards the top of the lungs. The results of applying the gradient function presented in Figure 8.1 show a reduction in blood flow as the vector parameter a goes from -30 to -200.

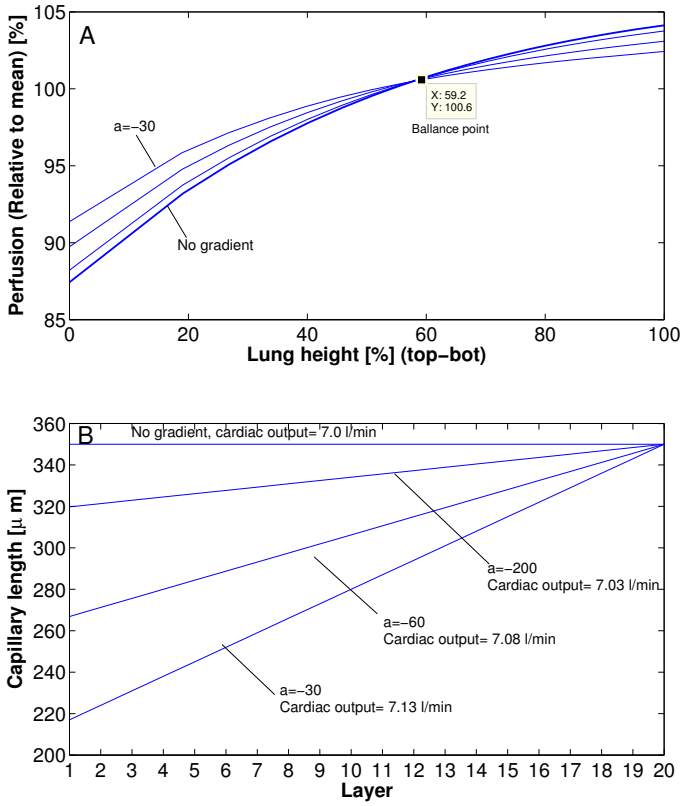

Figure 8.3: *Simulation results of using linear increasing gradients by the gradient function* `trimf()` *for the capillary length. The used gradient vector is: [a 20 20], where a=-30, a=-60, and a=-200.*

The opposite direction of the linear gradients on perfusion distribution down the lungs is investigated, as well. The gradients are presented in Figure 8.4. The used gradient vector is: [1 1 c], where c=50, c=80, and c=220. The results of applying the linear decreasing gradients of the capillary number and length are shown in Figure 8.5 and Figure 8.6, respectively.

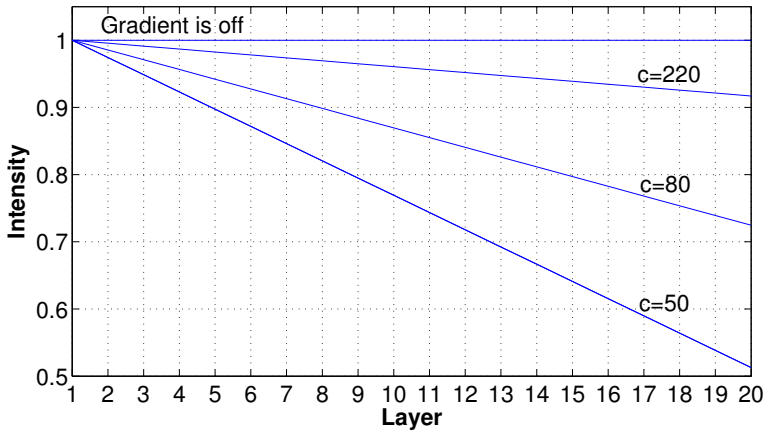

Figure 8.4: *The gradient function* `trimf()` *of the vector : [1 1 c]* where c parameter is specified to be 40,70, and 220.

In Figure 8.5A, the result of using decreasing gradient of capillary number is shown, where the cardiac output increases from 5.62 (c=50) to 7.0 (no gradient). The influence of gradients on the number of capillaries and cardiac output is shown in Figure 8.5B.

Furthermore, the effect of applying capillary length gradients with decreasing slopes are investigated, as well. In Figure 8.6A, the perfusion curve is slightly varied as a consequence of changing capillary number gradient. The cardiac output is thus changed from 7.09 (c=50) to 7.0 (no gradient) .

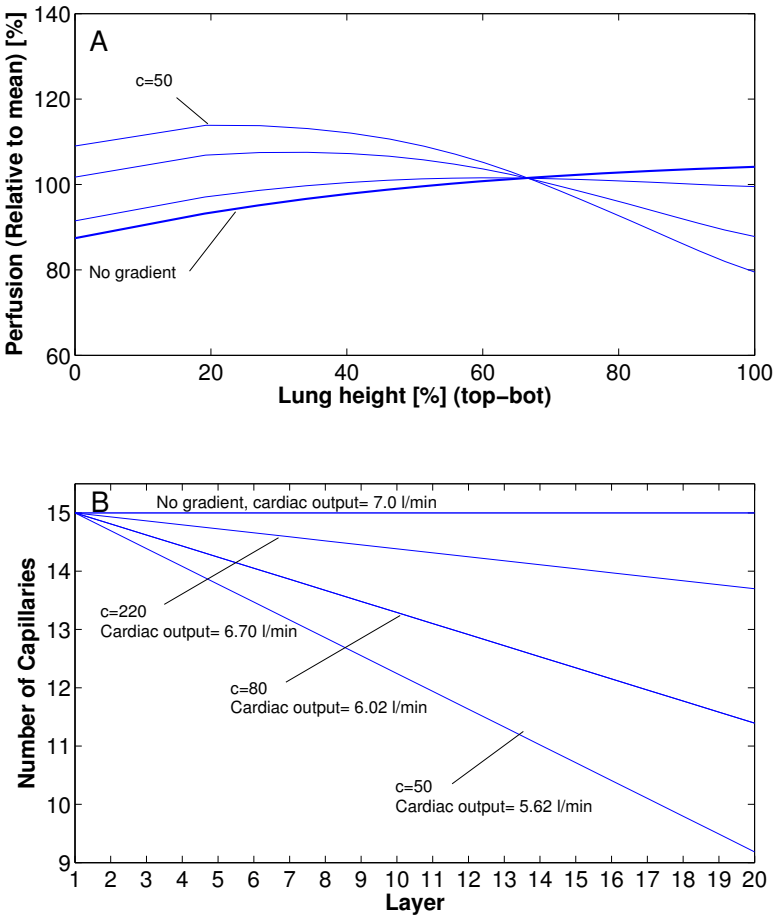

Figure 8.5: *The results of applying decreasing gradient of capillary number by the gradient function* `trimf()` *of the vector : [1 1 c]* where c parameter is specified to be 40, 70, and 220.

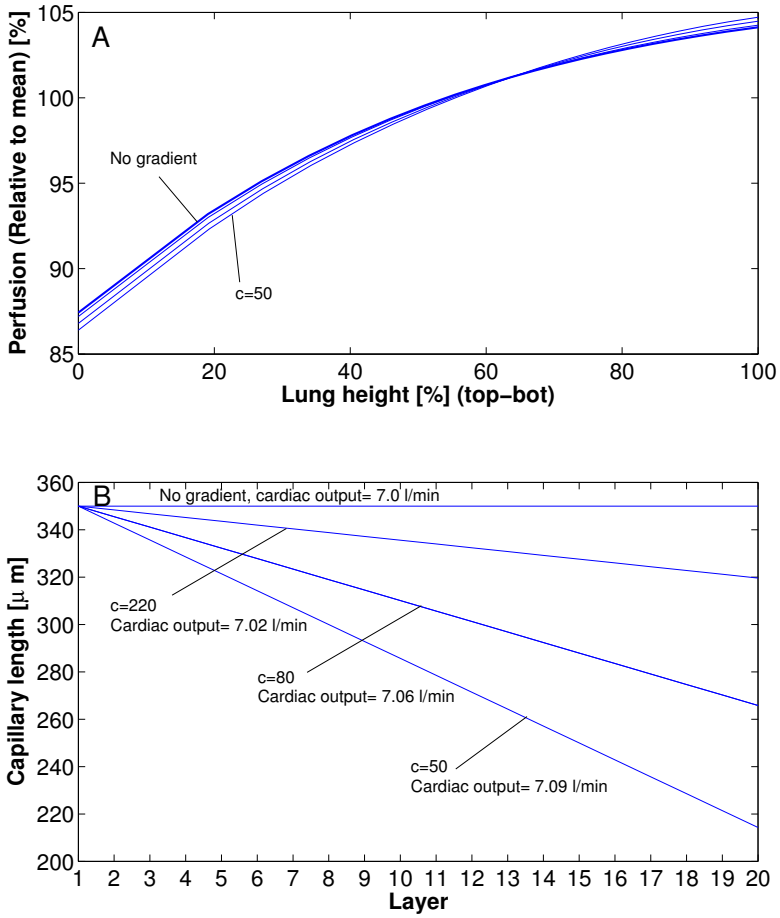

Figure 8.6: *The result of applying decreasing gradient of capillary number (Figure B) by the gradient function* `trimf()` *of the vector : [1 1 c]* where c parameter is specified to be 40, 80, and 220. Figure (A) shows simulations of perfusion for the respective gradient vectors.

8.1.2 Curved gradients

Based on the result from the linear gradients, it is shown that the number of capillaries surrounding the alveolar is much decisive than the length in the perfusion model. Therefore, the capillary length is evaluated to have a slight or negligible effect on perfusion distribution and decided not to use it in the remainder of this test.

When starting adjusting the simulation curve of the perfusion, it is convenient to have a fitted curve to the experimental data that can help with navigating the best fit. In addition, the coefficient of determination R^2 is used to determine how well the curve is fitted to the experimental data. The value of R^2 range from 0 to 1, where R^2=1 means a perfect correlation. To measure the error or difference between measured and estimated data, the error function root-mean square error (RMSE) is applied, as well. The strategy for finding the best fit to the experimental data by using the gradient function `pimf()`, is as follows:

- Starting with applying steep gradient of capillary number at lungs' peripheries, increasing toward the center.
- Finding the best possible fit to the experimental data by Jones et al. (2001) by adjusting the capillary number gradient along a fitted curve by MATLAB program.
- Finally, varying the maximum number of capillaries, N_{CapMax} while holding gradient vector of the curved function constant.

Results

The simulation results of applying the curved function `pimf`() are presented in Figure 8.7. The figure shows simulations which are yielded form applying three different gradient vectors: the first simulation, the used gradient vector is [-12 9 1.3 11,3]; the second simulation, the gradient vector [-20 8 9 70] is applied; the third simulation, the gradient vector [-8 9 11.3 60] is utilized which provides a reasonable fit (R^2=0.1908, RMSE=31.34%) to the experimental data compared with the fitted curve (red line, R^2=0.215, RMSE= 31.11 %). For each curve, R^2, RMSE in %, and cardiac output are presented.

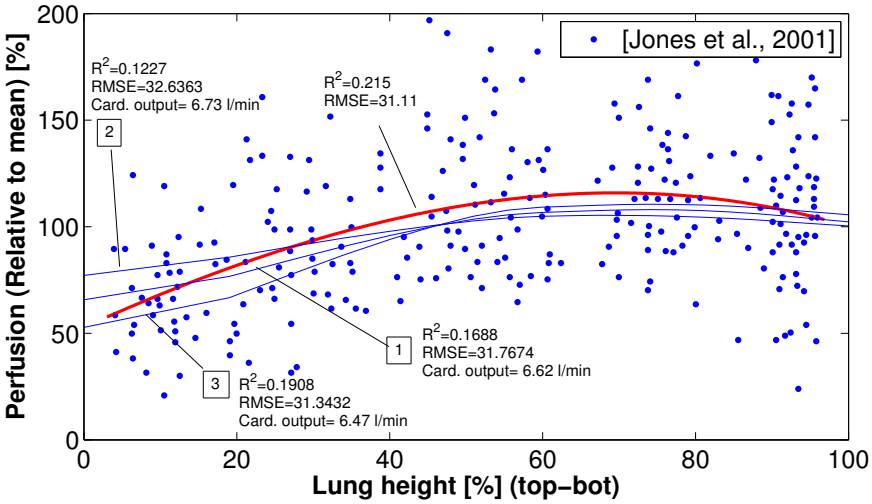

Figure 8.7: *Simulation results acquired by applying the curved gradient function. The figure presents three plots as well as a fitted curve (red line) to experimental data by Jones et al. (2001). For each curve, R^2, RMSE, and cardiac output is computed.*

Changing the value of N_{CapMax} has a negligible effect on simulation of perfusion down the lungs. The results of changing this parameter and its related cardiac output are presented in table 8.2.

N_{CapMax}	Cardiac output
15	6.45 l/min
17	7.33 l/min
20	8.63 l/min

Table 8.2: Changing the N_{CapMax} result in different cardiac values.

The highest R^2 can obtained is at gradient function vector of [-8 9 11.3 60], and with RMSE=31.3432. The best fit obtained by the gradient function is presented in Figure 8.8. This curve will be used in the next chapter to examine perfusion distribution at inverted body position.

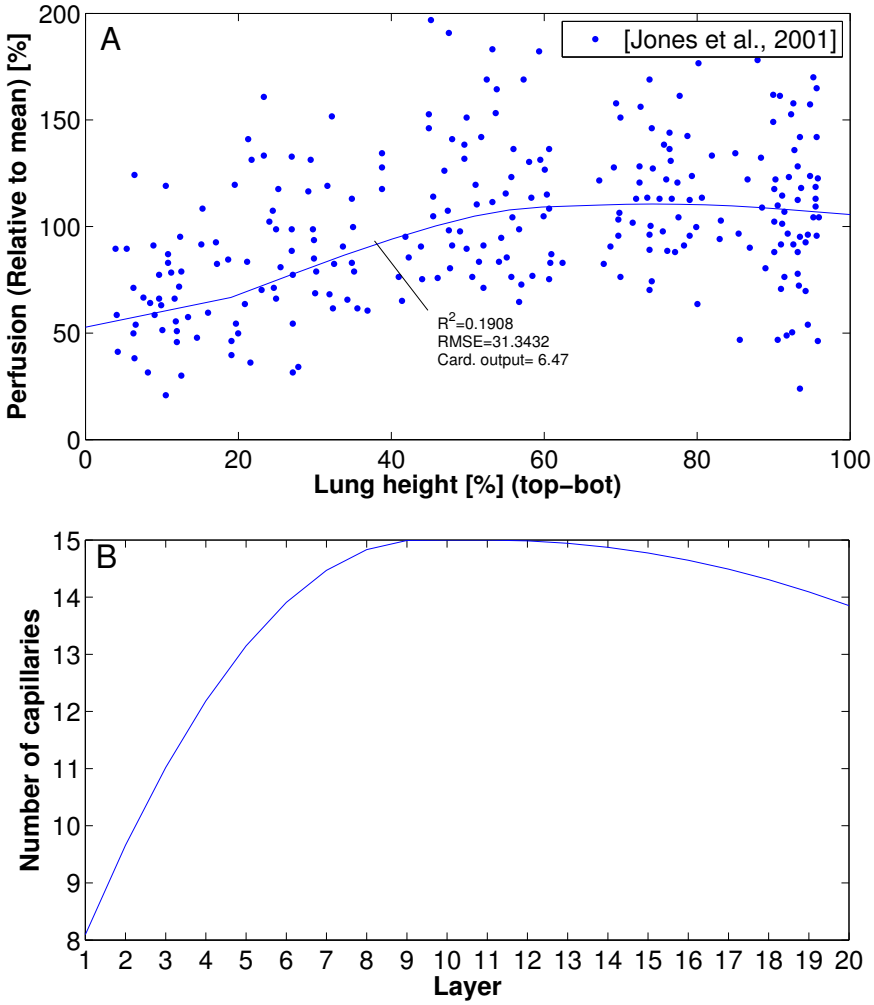

Figure 8.8: *A: simulation of perfusion utilizing the gradient vector [-8 9.3 11 57] from top (ventral part) to bottom (dorsal part) of the lungs. B: the number of capillaries as a function of layer index is presented for the belonging gradient vector. The gradient vector provides a reasonable fit to the experimental data by Jones et al. (2001).*

Part IV

Studying the Effect of Anatomical Gradient

Chapter 9

Studying the Effect of Anatomical Gradient in the prone posture

In order to examine how well the implemented anatomical gradient can describe perfusion distribution down the lung, simulation of blood flow distribution in prone posture will be performed. The simulation result from the inverted posture in comparison to supine posture will be presented and described in details.

Objective

The purpose of this study is to test the following hypothesis: *anatomical differences in the lungs contribute to heterogeneity of pulmonary perfusion.*

In order to test this hypothesis, a simulation of pulmonary perfusion in the prone posture will be carried out. A number of studies which investigated distribution of perfusion in supine and prone postures showed either significant [Mure and Lindahl, 2008, Prisk et al., 1994] or no change [Jones et al., 2001, Musch et al., 2002] in perfusion distribution between the two postures, see section 2.2.2. In these studies, heterogeneity pattern in both postures was a reduction in perfusion distribution towards the lung peripheries. The idea is thus to examine if an implemented anatomical gradient in supine can cause a reasonable heterogeneity pattern when changing body posture from supine to prone.

9.1 Assumptions

In order to examine the aim of this study, a number of assumptions are carried, which are listed in the following:

- It is assumed that distribution of perfusion is only affected by gravity and by an anatomical gradient due to the number of capillaries surrounding the alveolus.

- It is assumed that changing position from supine to prone has not effect on the form of lung profile.
- it is assumed that the lung mechanics is the same in both postures.

9.2 Method

In order to be able to test the hypothesis, a lung profile of the lungs' cross sectional areas as a function of lung depth in the prone posture will be applied. The profile is reconstructed from a supine lung profile using MATLAB program, which was computed by Mogensen et al. (2010). The lung profile in prone and supine postures are shown in Figure 9.1A and Figure 9.1B, respectively.

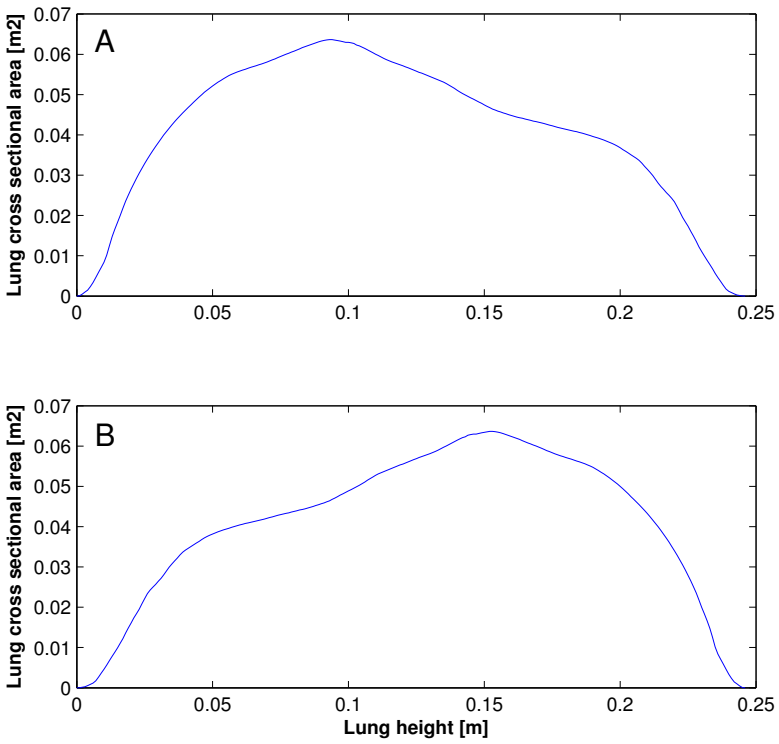

Figure 9.1: *Lung profile for a subject in (A) the prone and (B) supine postures, presenting the lung cross sectional area as a function of lung depth. The lung depth at zero represent the ventral part of the lungs in Figure (A), whereas in Figure (B) represents the dorsal part of the lungs.*

Changing posture from supine to prone requires inverting the gradient of capillary number to prone posture. The gradient of capillary number is presented in Figure 9.2.

The gradient vector of the gradient function `pimf()` for prone position will be thus [-36 10 11.7 29].

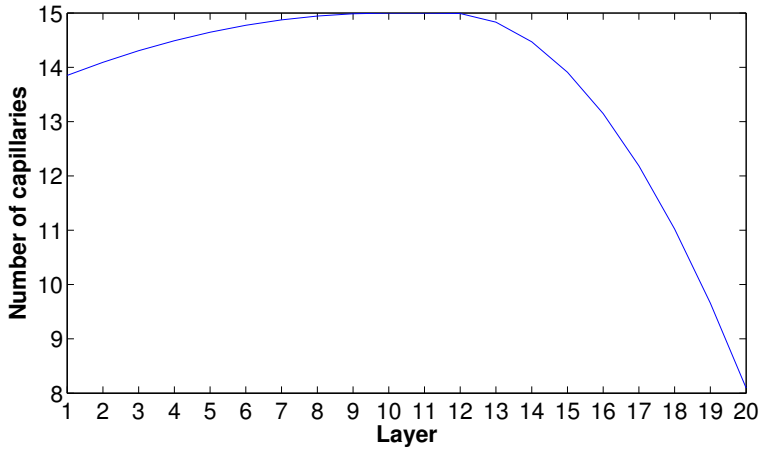

Figure 9.2: *A plot of the capillary number as a function of layer index for prone posture using the gradient function* `pimf()` *with the vector: [-36 10 11.7 29]*

The simulation of perfusion is dependent on constant values as specified in table 9.1.

Parameter	Value	Description
L_{CapMax}	350 μm	The maximum length of alveolar capillary
N_{CapMax}	15	The maximum number of capillaries per alveolus
N_{Layer}	20	The number of lung layers
$Resolution$	30	Number of pressure step in a breath
$N_{Breaths}$	2	Number of breaths

Table 9.1: The values of the used parameters and their description.

9.3 Results

The simulation of perfusion down the lung for a subject in the prone posture versus supine posture is shown in Figure 9.3. The simulation of perfusion in the prone posture shows an increase in blood flow distribution in the non-dependent lung regions. In the most dependent lung region, a significant decrease in perfusion is presented. In addition, the cardiac output is slightly reduced from 6.47 l/min in supine to 6.30 l/min in prone.

The applied curved gradient function in the supine position (see Figure 8.8) provides an steep slope with increasing in number of capillaries from the non-dependent to the center of the lungs, thereafter decreases slightly towards the dependent lung regions. When changing position from supine to prone, the same gradient function is utilized, but in inverted direction, see Figure 9.2. This causes an opposite effect on perfusion distribution, where perfusion becomes approximately linear in the non-dependent lung regions. However, in the dependent lung regions the perfusion is reduced significantly. The results show perfusion distribution that ranges in the same interval form approximately 54% to 90% in perfusion axis for both postures.

The results of implementing the anatomical gradient due to number of capillaries show a reasonable data for prone posture according to supine posture. This may imply that anatomical gradients describing distribution of blood flow down the lung from dependent to non-dependent to dependent lung regions.

The reduction in perfusion distribution in the dependent an non-dependent lung regions can be explained by gravity. That is, changing position from supine to prone make the distribution of perfusion more homogeneous in the non-dependent lung regions and the lung centers, where simulation curve becomes linear. In the dependent lung regions . Decreasing the perfusion in the non-dependent lung regions can be described by the gravity been more compressed

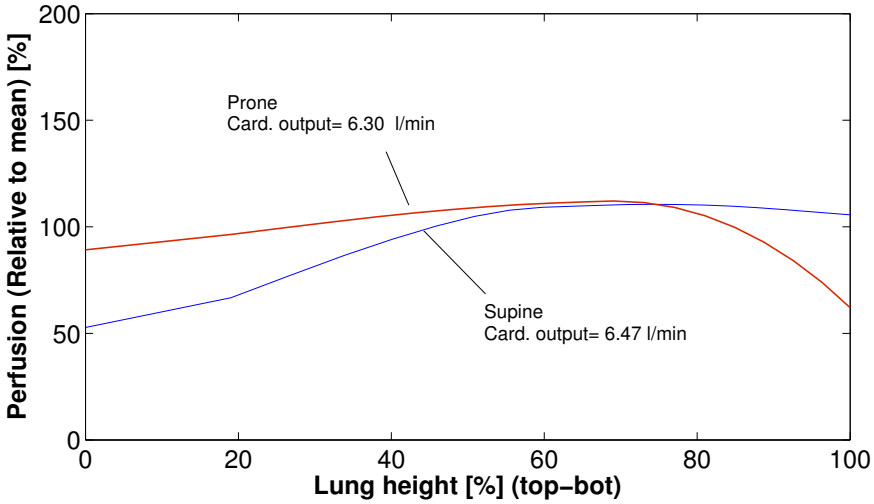

Figure 9.3: *Simulation of perfusion in prone posture (red line) vs. supine (blue line) from non-dependent (top) to dependent regions of the lungs. Note that the top at depth=zero is ventral in supine, where in prone is dorsal part of the lungs.*

Part V

Synthesis

Chapter 10

Discussion

The aim of this chapter is to discuss some of the model assumptions, assumption for implementing the anatomical gradients, results of the sensitivity analysis, and result of studying anatomical gradients in prone posture.

10.1 Assumptions

In the following there will be discussed a number of assumptions that have been made by Mogensen et al. (2010), and assumptions for implementing the anatomical gradients into the perfusion model.

Assumptions for implementing the gradients

For implementing the anatomical gradients, three assumptions are made. These assumptions are discussed in the following:The assumptions that are made for studying perfusion distribution in prone posture are in the following:

- *Pulmonary capillaries differ in number and length from top to bottom of the lungs.* This assumption is made to investigate what anatomical differences that contribute to perfusion heterogeneity in the lungs. Studies which investigated pulmonary perfusion suggested differences due to geometry and branching of vascular tree. It is however not clear in the investigated literature how anatomical differences can contribute to distribution of perfusion.

  One way to investigate this hypothesis is by simulating perfusion distribution down the lungs due to changes in a given number of anatomical parameters. This project make use of two anatomical parameters, namely the length and number of capillaries surrounding the alveoli.

- *There is a gradient describing the number and length of the pulmonary capillaries.* The assumption is made for describing the pattern of blood flow distribution in the lungs using a gradient function. However, the distribution of these two parameters is not described by any of the examined studies nor the office knowledge on lung physiology explain these parameters.

Assumptions for studying the effect of anatomical gradients in prone posture

- *The distribution of pulmonary perfusion is only affected by anatomical gradient and gravity.* The distribution of perfusion can be affected by a number of active and passive mechanisms. The active mechanisms match local ventilation and perfusion by altering the pulmonary vascular resistance, among others. In healthy human lungs, measuring regional distribution of perfusion in a subject, breathing room-air with 30% and 12.5% oxygen failed to find a significant change [Arai et al., 2009]. Recently, the active mechanisms are reported by [Glenny and Robertson, 2011] to have a negligible effect on perfusion distribution in healthy human lungs, leaving only the passive mechanisms due to gravity and anatomical differences in the lungs. In this project, the simulation of perfusion is done for healthy human lungs, it is therefore reasonable to assume no contribution from active mechanisms.

- *The lung profile is the same in supine and prone.* This can be one of the limitations for simulation of perfusion in prone position. Changing posture from supine to prone would have an effect on the shape of the lungs, and thus the cross-sectional area. Measurements of the lungs in both postures using MRI indicated that the central posterior portions more compressed in supine than were the central anterior portions. This might be attributed to the weight of the heart and influences of the adjacent structures. [Prisk et al., 1994]. However, the model does not include the effect of heart weight and the surrounding tissues on the lungs in supine posture.

- *Lung mechanics in supine and prone* Because the simulation of pulmonary perfusion is performed for subject holding breath, the lung mechanics is assumed to be not affected by the posture.

10.2 Results

In the following there will be discussed the results of the sensitivity analysis and results of studying the effect of implementing the anatomical gradients in prone posture.

Sensitivity Analysis

The sensitivity analysis is divided into two parts. The first part is performed using linear gradients, whereas the second part is conducted using curved gradients.

Applying linear gradients of capillary number results in changes in the simulations of perfusion and cardiac output, (see e.g. Figure 8.2). The resulted curves of perfusion intersect in a fixed point in the lungs, where perfusion is constant independent on the slope of the applied gradients. The blood distribution before and after the fixed point is balanced in the way that if blood is reduced in the non-dependent regions, it will increase in the dependent regions of the lungs. This may indicate a constant flow in the center of the lungs even with large number of capillaries.

Using curved gradient function enables to describe the pattern of blood flow distribution in the lungs. The curved gradient function is feasible in the sense that its resultant curve can be reconstructed easily, adjusting its parameters.

Studying the Effect of Anatomical Gradient in the Supine Posture

The result of implementing an anatomical gradient due to the number of capillaries in prone position is shown in Figure 9.3. The simulation results present a reduction in perfusion distribution in the dependent lung regions, which is in agreement with the experimental result form e.g. [Prisk et al., 1994] for healthy human subjects (2.7). The result shows a reasonable distribution pattern with almost equal range of perfusion as in supine position, and a slight difference in cardiac output. The study is therefore in agreement with studies in that there are anatomical gradient describing distribution of perfusion.

10.3 Limitions

Limitations in this project are discussed in the following:

The capillary model

The alveolar three types of capillaries are approximated with one-capillary model. This approximation allows to simplify modeling the alveolar capillaries. The number and length of the modeled capillaries are thus not related to the number and length of the real capillaries.

Choosing the anatomical parameters

This project makes use only of two anatomical parameters, which are the number and length of capillaries, investigating the influence of anatomical gradients due to changes

in these parameters in the lungs. Other anatomical parameters which might contribute to distribution of perfusion is the bifurcation of the vascular tree and the pattern of the branching. A model of vascular tree was modeled by [Huang et al., 1996] basing on morphometric data from human vascular tree. However the model is lacking of describing different elements such as the elasticity of vessels and branching angle.

Calibrating the perfusion model

The experimental data from Jones et al. (2001) is used for calibrating the model simulation. The experimental data is in agreement with other findings e.g. [Glenny et al., 1991, Glenny et al., 1999, Prisk et al., 1994] that showed a reduction in zone 4 of the lungs, which is hypothesized to be due to some anatomical differences in the lungs. However, other experimental data do not show a reduction of perfusion in zone 4, e.g. [Brudin et al., 1994] who measured perfusion distribution per $cm3$ of lung tissue. It is difficult to evaluate which data is best for calibrating the model. However, to generalize the results from implementing the anatomical gradients, the calibrated model of perfusion should be able to describe the trend of other experimental data.

Validation of results in prone posture

The result of this study is not validated against an experimental data. To do so, an experimental data by [Jones et al., 2001] for healthy subjects in prone posture can be applied. However, Jones et al. (2001) measured no significant difference between supine and prone postures.

Lung profile in prone posture

Another limitation is due to lack of available experimental data for this study. The study uses an inverted lung profile for a subject in supine posture, which could affect the result of the study. This limitation is explained under "Assumptions for studying the effect of anatomical gradients in prone posture"

10.4 Implications of the results

The results of this study may indicate that anatomical gradients in the lungs are responsible for distribution of perfusion. The results, however need to be validated against an experimental data. In addition, a lung profile for subject in the prone posture has to be constructed to ensure a valid results.

10.5 Future work

Topics for future work could be finding and investigating the effect of implementing new anatomical parameters on simulation of the perfusion model, as well as examining the effect of implementing a model of vascular tree in the perfusion model.

Chapter 11

Conclusion

Initially, a clinical background for this project is presented describing the problem of Acute Respiratory Distress Syndrome and Acute Lung Injury in the intensive care unit. Thereafter, the project focusses on healthy human lungs to understand the problem of perfusion heterogeneity. The pattern of pulmonary perfusion distribution is hypothesized to be caused by a number of anatomical parameters, such as the geometry and pattern of vascular tree. This project make use of the perfusion model by Mogensen et al. (2010) to investigate the problem statement which is shown in the following.

- *How is it possible to implement anatomical gradients in the model by Mogensen et al. (2010) to obtain a correct reflection of perfusion distribution? How can this help with providing better understanding of the mechanisms that contribute to perfusion heterogeneity in healthy human lungs?*

The first part of the problem statement is solved by implementing two gradient functions, linear and curved gradient functions. The linear gradient function is used to conduct a sensitivity analysis, whereas the curved function is used to calibrate the model to fit an experimental data by Jones et al. (2001). The best fit to the experimental data as well as its corresponding cardiac output are calculated. In addition an error function is used.

The second part of the problem statement is answered by investigating *In silico* the hypothesis that "the anatomical differences in the lungs contribute to heterogeneity of pulmonary perfusion". The experiment is conducted in the prone posture and compared with supine posture. The results of the experiment is in agreement with experimental data measured in supine and prone postures in indicating a pattern of perfusion due to anatomical gradients.

Bibliography

[A.B. Millar, 1989] A.B. Millar, D. D. (1989). Vertical gradients of lung density in healthy supine men. Thorax *44*, 485–490.

[Amato et al., 1998] Amato, M. B. P., Barbas, C. S. V., Medeiros, D. M., Magaldi, R. B., Schettino, G. D. P. P., Lorenzi-Filho, G., Kairalla, R. A., Deheinzelin, D., Munoz, C., Oliveira, R., Takagaki, T. Y. and Carvalho, C. R. R. (1998). Effect Of A Protective-Ventilation Strategy On Mortality In The Acute Respiratory Distress Syndrome. The New England Journal of Medicine *338(6):347-354*.

[Amis et al., 1984] Amis, T., Jones, H. A. and Hughes, J. (1984). Effect of posture on inter-regional distribution of pulmonary perfusion and V[combining dot above]aQ[combining dot above] ratios in man. Respiration Physiology *56*, 169 – 182.

[Andreassen et al., 2010] Andreassen, S., Steimle, K. L., Mogensen, M. L., de la Serna, J. B., Rees, S. and Karbing, D. S. (2010). The effect of tissue elastic properties and surfactant on alveolar stability. Journal of Applied Physiology *109:1369–1377*.

[Angus and Thurbeck, 1972] Angus, G. and Thurbeck, W. (1972). Number of alveoli in the human lung. Journal of Applied Physiology *32: 483–485*.

[Arai et al., 2009] Arai, T. J., Henderson, A. C., Dubowitz, D. J., Levin, D. L., Friedman, P. J., Buxton, R. B., Prisk, G. K. and Hopkins, S. R. (2009). Hypoxic pulmonary vasoconstriction does not contribute to pulmonary blood flow heterogeneity in normoxia in normal supine humans. Journal of Applied Physiology *106*, 1057–1064.

[Brower et al., 2004] Brower, R. G., Lanken, P. N., MacIntyre, N., Matthay, M. A., Morris, A., , Ancukiewicz, M., Schoenfeld, D. and Thompson, B. T. (2004). Higher versus Lower Positive End-Expiratory Pressures in Patients with the Acute Respiratory Distress Syndrome. New England Journal of Medicine *351(4):327-336*.

[Brower et al., 2000] Brower, R. G., Matthay, M. A., Morris, A., Schoenfeld, D., Thompson, B. T. and Wheeler, A. (2000). Ventilation With Lower Tidal Volumes As Compared With Traditional Tidal Volumes For Acute Lung Injury And The Acute

Respiratory Distress Syndrome. the Massachusetts Medical Society *342(18):1301-1208*.

[Brudin et al., 1994] Brudin, L. H., Rhodes, C. G., Valind, S. O., Jones, T., Jonson, B. and Hughes, J. M. (1994). Relationships between regional ventilation and vascular and extravascular volume in supine humans. J Appl Physiol *76*, 1195–1204.

[Chiumello et al., 2008] Chiumello, D., Carlesso, E., Cadringhe, P., Caironi, P., Valenza, F., Polli, F., Tallarini, F., Cozzi, P., Cressoni, M., Colombo, A., Marini, J. J. and Gattinoni, L. (2008). Lung Stress and Strain during Mechanical Ventilation for Acute Respiratory Distress Syndrome. Respir and critical care *178(4):346-355*.

[Dale et al., 1980] Dale, P. J., Matthews, F. L. and Schroter, R. C. (1980). Finite element analysis of lung alveolus. Journal of Biomechanics *13*, 865–873.

[Despopoulos and Silbernagl, 2003] Despopoulos, A. and Silbernagl, S. (2003). Color Atles of Physiology. ISBN:3-13-545005-8, fifth edition, Georg Thieme Verlag.

[Ferner and Staubesand, 1982] Ferner, H. and Staubesand, J. (1982). Sobotta Atlas of Human Anatomy. Urban & Schwarzenberg.

[Galvin et al., 2007] Galvin, I., Drummond, G. B. and Nirmalan, M. (2007). Distribution of blood flow and ventilation in the lung: gravity is not the only factor. British Journal of Anaesthesia *(4): 420–8*.

[Girard and Bernard, 2010] Girard, T. D. and Bernard, G. R. (2010). Mechanical Ventilation in ARDS. Chest Journal *131:921-929*.

[Glenny et al., 1991] Glenny, R., Lamm, W., Albert, R. and Robertson, H. (1991). Gravity is a minor determinant of pulmonary blood flow distribution. J Appl Physiol *7*, 620–9.

[Glenny et al., 1999] Glenny, R. W., Bernard, S., Robertson, H. T. and Hlastala, M. P. (1999). Gravity is an important but secondary determinant of regional pulmonary blood flow in upright primates. J. Appl. Physiol. *86(2):623–632*.

[Glenny et al., 2000] Glenny, R. W., Lamm, W. J. E., Bernard, S. L., An, D., Chornuk, M., Pool, S. L., Wagner, W. W., Jr, Hlastala, M. P. and Robertson, H. T. (2000). Physiology of a Microgravity Environment Selected Contribution: Redistribution of pulmonary perfusion during weightlessness and increased gravity. J Appl Physiol *89*, 1239–1248.

[Glenny and Robertson, 2011] Glenny, R. W. and Robertson, H. T. (2011). Spatial Distribution of Ventilation and Perfusion: Mechanisms and Regulation. John Wiley and Sons, Inc.

[Gregory and Marshall, 2003] Gregory, D. and Marshall, D. (2003). Wellcome Images. Scanning electron micrograph. Lastchecked:25.08.2011. `http://images.wellcome.ac.uk/`.

[Hakim et al., 1988] Hakim, T. S., Dean, G. W., and Lisbona, R. (1988). Effect of body posture on spatial distribution of pulmonaryblood flow. J Appl Physiol *64*, 1160–70.

[Hakim et al., 1987] Hakim, T. S., Lisbona, R. and Dean, G. W. (1987). Gravity-independent inequality in pulmonary blood flow in humans. Journal of Applied Physiology *63*, 1114–1121.

[Hamid et al., 2005] Hamid, Q., Shannon, J. and Martin, J. (2005). Physiologic basis of respiratory disease. illustrated edition, BC Decker, Inc.

[Hickling, 1998] Hickling, K. G. (1998). The Pressure-Volume Curve Is Greatly Modified by Recruitment. Am. J. Respir. Crit. Care Med. *158(1):194-202*.

[Huang et al., 1996] Huang, W., Yen, R. T., McLaurine, M. and Bledsoe, G. (1996). Morphometry of the human pulmonary vasculature. Journal of Applied Physiology *81*, 2123–2133.

[Hughes et al., 1968] Hughes, J. M. B., Glazier, J. B., Maloney, J. E. and West, J. B. (1968). Effect of lung volume on the distribution of pulmonary blood flow in man. Respiration Physiology *4:58-72*.

[Jones et al., 2001] Jones, A. T., Hansell, D. M. and Evans, T. W. (2001). Pulmonary perfusion in supine and prone positions: an electron-beam computed tomography study. J Appl Physiol *90:1342–1348*.

[Kansal, 2004] Kansal, A. R. (2004). Modeling Approaches to Type 2 Diabetes. Diabetes Technology and Therapeutics *6(1): 39-47*.

[Kenner, 1989] Kenner, T. (1989). The measurement of blood density and its meaning. Basic. Res. Cardiol. *84*, 111–124.

[Lambert et al., 1982] Lambert, R., Wilson, T., Hyatt, R. and Rodarte, J. (1982). A computational model for expiratory flow. J Appl Physiol *1*.

[Letner, 2005] Letner, C., ed. (2005). Geigy Scientific Tables: Heart and Circulation, vol. 5, of 0-914168-54-1. Ciba Pharmaceutical Co.

[Levin et al., 2001] Levin, D. L., Chen, Q., Zhang, M., Edelman, R. R. and Hatabu, H. (2001). Evaluation of Regional Pulmonary Perfusion Using Ultrafast Magnetic Resonance Imaging. Magnetic Resonance in Medicine *46:166–171*.

[Lewis et al., 1970] Lewis, M. L., Gnoj, J., Fisher, V. J. and Christianson, L. C. (1970). Determinants of pulmonary blood volume. J Clin Invest. *49*, 170–182.

[Liu et al., 1998] Liu, C., Niranjan, S., Jr., J. C., San, K., Zwischenberger, J., Niranjan, A. B. S., Jr., J. C., San, K., Zwischenberger, J. and Bidani, A. (1998). Airway mechanics, gas exchange, and blood flow in a Nonlinear Model Of The Normal Human Lung. J Appl Physiol *84*, 1447–1469.

[Lumb, 2005] Lumb, A. B. (2005). Nunn's Applied Respiratory Physiology. ISBN:978-0-7506-8791-1, Elsevier.

[MacIntyre, 2000] MacIntyre, N. R. (2000). Mechanical Ventilation Strategies for Lung Protection. Thieme Medical Publishers *21(3):205-222*.

[Martini, 2005] Martini, F. H. (2005). Fundamentals of Anatomy & Physiology. 0-8053-7280-6, Benjamin-Cummings Publishing Company.

[McCance and Huether, 2006] McCance, K. L. and Huether, S. E. (2006). Pathophysiology: The Biologic Basis for Disease in Adults and Children. 13:978-0-323-03507-1 and 10:0-323-03507-8, fifth edition, Elsevier Mosby.

[Meade et al., 2008] Meade, M., Cook, D., Guyatt, G., Slutsky, A., Arabi, Y., Cooper, D., Davies, A., Hand, L., Zhou, Q., Thabane, L., Austin, P., Lapinsky, S., Baxter, A., Russell, J., Skrobik, Y., Ronco, J. and Stewart, T. (2008). Ventilation strategy using low tidal volumes, recruitment maneuvers, and high positive end-expiratory pressure for acute lung injury and acute respiratory distress syndrome: a randomized controlled trial. JAMA *299(6):637-45*.

[Mercat et al., 2008] Mercat, A., Richard, J., Vielle, B., Jaber, S., Osman, D., Diehl, J., Lefrant, J., Prat, G., Richecoeur, J., Nieszkowska, A., Gervais, C., Baudot, J., Bouadma, L. and Brochard, L. (2008). Positive end-expiratory pressure setting in adults with acute lung injury and acute respiratory distress syndrome: a randomized controlled trial. JAMA *299(6):646-55*.

[Mogensen et al., 2010] Mogensen, M., Steimle, K., Karbing, D. and Andreassen, S. (2010). A model of perfusion of the healthy human lung. Comput Methods Programs Biomed *101(2):156-65*.

[Mure and Lindahl, 2008] Mure, M. and Lindahl, S. G. E. (2008). Prone position improves gas exchange – but how? Acta anaesthesiologica scandinavica *45*, 150–159.

[Musch et al., 2002] Musch, G., Layfield, J. D. H., Harris, R. S., Melo, M. F. V., Winkler, T., Callahan, R. J., Fischman, A. J. and Venegas, J. G. (2002). Topographical distribution of pulmonary perfusion and ventilation, assessed by PET in supine and prone humans. J Appl Physiol *93*, 1841–185.

[Nyrén et al., 1999] Nyrén, S., Mure, M., Jacobsson, H., Larsson, S. A. and Lindahl, S. G. E. (1999). Pulmonary perfusion is more uniform in the prone than in the supine position: scintigraphy in healthy humans. J Appl Physiol *86*, 1135–1141.

[Phua et al., 2009] Phua, J., Badia, J. R., Adhikari, N. K. J., Friedrich, J. O., Fowler, R. A., Singh, J. M., Scales, D. C., Stather, D. R., Li, A., Jones, A., Gattas, D. J., Hallett, D., Tomlinson, G., Stewart, T. E., and and, N. D. F. (2009). Has Mortality from Acute Respiratory Distress Syndrome Decreased over Time? American journal of respiratory critical care *179(14):220-227*.

[Pries et al., 1996] Pries, A., Secomb, T. and Gaehtgens, P. (1996). Biophysical aspects of blood flow in the microvasculature. cardiovasc Res. *32*, 654–67.

[Prisk et al., 1994] Prisk, G., Guy, H., Elliott, A. and West, J. (1994). Inhomogeneity of pulmonary perfusion during sustained microgravity on SLS-1. J Appl Physiol *76(4):1730-8*.

[Prisk et al., 2007] Prisk, G. K., Yamada, K., Henderson, A. C., Arai, T. J., Levin, D. L., Buxton, R. B. and Hopkins, S. R. (2007). Pulmonary perfusion in the prone and supine postures in the normal human lung. J Appl Physiol *103*, 883–894.

[Rhoades and Bell, 2009] Rhoades, R. A. and Bell, D. R. (2009). Medical physiology: preinciples for clinical medicine. 13:978-0-7817-6852-8, third edition, Wolters Kluwer.

[Robertson, 2009] Robertson, H. T. (April 2009). Does hypoxic vasoconstriction influence the normal distribution of human pulmonary blood flow? Journal of Applied Physiology *106*, 1034–1035.

[Rotta, 2006] Rotta, A. T. (2006). Lung-protective ventilation in pediatrics. US RESPIRATORY CARE .

[Schraufnagel and Schmid, 1988] Schraufnagel, D. E. and Schmid, A. (1988). Capillary structure in elastase-induced emphysema. Am J Pathol. *130*, 126–135.

[Silverthorn, 2001] Silverthorn, D. U. (2001). Human physiology: an integrated approach. Prentice Hall.

[Sobin et al., 1972] Sobin, S. S., Fung, Y. C., Tremer, H. M. and Rosenquist, T. H. (1972). Elasticity of the Pulmonary Alveolar Microvascular Sheet in the Cat. Circ Res. *30*, 440–50.

[Soni and Williams, 2008] Soni, N. and Williams, P. (2008). Positive Pressure Ventilation: What is the Real Cost?: Ventilation, Alveolar Ventilation, and Recruitment. `http://www.medscape.com/viewarticle/581344_4`.

[Steimle et al., 2010] Steimle, K., Mogensen, M., Karbing, D., Bernardino, de la Serna, J. and Andreassen, S. (2010). A model of ventilation of the healthy human lung. Comput Methods Programs Biomed *101*, 144–5.

[Tobin and Kelly, 1999] Tobin, A. and Kelly, W. (1999). Prone ventilation–it's tim. Anaesth Intensive Care *27*, 194–201.

[Venegas et al., 1998] Venegas, J. Ì. G., Harris, R. S., and Simon, B. A. (1998). A comprehensive equation for the pulmonary pressure-volume curve. Journal of Applied Physiolog *84(1):389-395*.

[Verbrugge et al., 2007] Verbrugge, S. J. C., Lachmann, B. and Kesecioglu, J. (2007). Lung protective ventilatory strategies in acute lung injury and acute respiratory distress syndrome: from experiment findings to clinical application. Clin Physiol Funct Imaging *27:67-90*.

[Voelkel and Rounds, 2009] Voelkel, N. and Rounds, S. (2009). The Pulmonary Endothelium: Function in Health and Disease. John Wiley and Sons.

[Walther et al., 2005] Walther, S. M., Johansson, M. J., Flatebø, T., Nicolaysen, A. and Nicolaysen, G. (2005). Marked differences between prone and supine sheep in effect of PEEP on perfusion distribution in zone II lung. Journal of Applied Physiology *99*, 909–914.

[West, 2002] West, J. B. (2002). Importance of gravity in determining the distribution of pulmonary blood flow. J Appl Physiol *93:1888-1891.*

[West et al., 1964] West, J. B., Dollery, C. T. and Naimark, A. (1964). Distribution of blood flow in isolated lung; relation to vascular and alveolar pressures. J Appl Physiol *19: 713–24.*

[Wilson and Bachofen, 1982] Wilson, T. A. and Bachofen, H. (1982). A model for mechanical structure of the alveolar duct. J Appl Physiol *52(2):1064-1070.*

Part VI

APPENDIX

Appendix A

The Ventilation Model

The aim of this chapter is to briefly describe the ventilation model designed by Steimle et al (2010).

A.1 The model of ventilation

The physiological model of ventilation described the lung mechanics and distribution of ventilation in the healthy human lungs. Modeling the lungs were achieved by dividing the lungs into number of horizontal layers. This made the model capable of simulating the local pressure-volume curve and ventilation at different depths of the lung. Figure A.1 demonstrates the overall structure of the model in which the lungs were divided into 10 layers for simplification. The input to the model was the airway pressure or alveolar pressure.

A.1.1 The model assumption

Designing the ventilation model were based on the following assumptions:

- Each layer was assumed to have the same number of alveoli.
- The density of air was assumed negligible.
- The airway resistance and viscoelasticity were assumed minimal during normal tidal breathing at rest.
- The pressure in pulmonary airways was assumed to distribute equivalently to all pulmonary alveoli.
- Since the model simulated a paralyzed subject during mechanical ventilation, the pressure contribution from muscles was assumed absent.

- The alveolus were assumed to have a spherical shape inflated by a rigid ring, an opening with constant radius equivalent in all alveoli.
- The alveoli were assumed to be equally sized when lung at the total lung capacity independent of lung size of the subject.
- The blood and tissue were assumed distributed equivalently between all the alveoli.
- It is assumed that the lungs expend isotropically and all subjects have the same lung profile.

A.1.2 Anatomy

The number of alveoli in layer i, $N_{AlvPrLayer}$, was found by dividing the total number of alveoli, N_A, by the number of layers, N_{Layers}, the lung were divided into, as stated in equation A.1.

$$N_{AlvPrLayer} = \frac{N_A}{N_{Layers}} \tag{A.1}$$

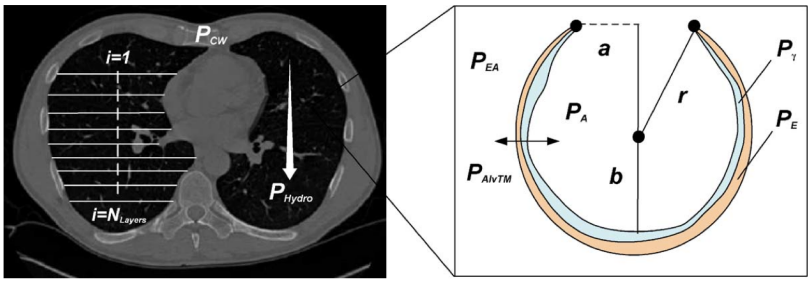

Figure A.1: *Schematic illustration the overall structure of the ventilation model. left, a computed tomographic image of the transverse plane for a subject in the supine position demonstrates the lungs as divided into 10 horizontal layers. The layer index (i) controls the layer depth which increments downwards.* P_{Hydro}*, hydrostatic pressure exerted by lung tissue and blood.* P_{EA}*, extraalveolar pressure.* P_{A}*, airway pressure.* P_{AlvTM}*, alveolar transmural pressure. Right, schematic illustration of the alveolar model. a, alveolar opening radius. b, distance from the opening to the bottom of the alveolus. r, alveolar radius. [Steimle* et al.*, 2010]*

In order to simulated the lung mechanics, the ventilation model included the following aspects:

Alveolar geometry: A model that describes alveolar geometric properties was incorporated in the ventilation model. The model represents the alveolus as a sphere with an opening, as shown in Figure A.2.

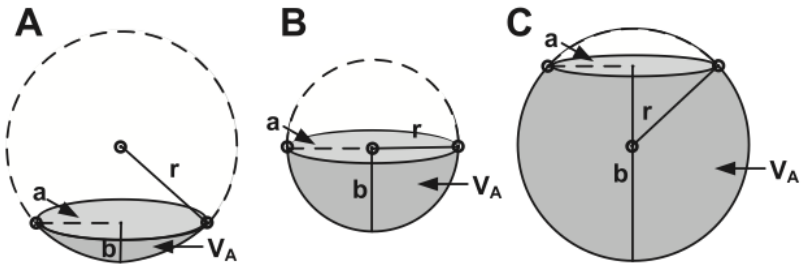

Figure A.2: *The geometric model of the alveolus. a, the opening radius of the alveolus. r, the alveolar radius. b, the height from the alveolar opening.* V_A*, volume of the alveolus at different radii. A: saucer shaped. B: a hemisphere. C: spherical shape. [Andreassen* et al.*, 2010]*

Pressure due to the chest wall: the pressure exerted by the chest wall, P_{CW} was calculated at different lung volume using equation. A.2.

$$P_{CW} = 0.071KPa - ln(\frac{95\%}{(V_{Air}/V_{TLC}) - 22\%} - 1) \cdot 0.58kPa \tag{A.2}$$

Where V_{Air} is the total volume of air in the lungs, whereas V_{TLC} is the total lung volume.

Pressure due to surface tension : The ventilation model included the effect of alveolar surface tension and surfactant on alveolar transmural pressure. The alveolar surface tension is calculated by Laplace equation as stated in equation A.3

$$P_{\gamma,i} = \frac{2 \cdot \gamma_i}{r_i} \tag{A.3}$$

Where γ_i is the surface tension of an alveolus in layer i, whereas r_i is the radius of the alveolus.

Pressure due to lung tissue elasticity : The elasticity of the lungs was included assuming that the lung tissue can resist collapse at negative transmural pressure. The pressure due to the lungs tissue elasticity, $P_{E,i}$, is computed in equation A.4

$$P_{E,i} = 0.36\ kPa - ln(\frac{1-\epsilon}{(V_{A,i}/V_{AMax}) - \epsilon} - 1) \cdot 0.3\ kPa \tag{A.4}$$

Where ϵ= -0.05, $V_{A,i}$ is the volume of the alveolus in layer i, V_{AMax} is the maximum volume of a single alveolus.

Pressure due to the hydrostatic effects of the lung tissue and blood : The hydrostatic pressure at a given depth down the lung is computed using equation A.5.

$$P_{Hydro,i} = \sum_{j=1}^{i-1} \cdot \rho_{Lung,j} \cdot t_j \tag{A.5}$$

Where $P_{Hydro,i}$ is the hydrostatic pressure of on layer i, $\rho_{Layer,j}$ is the density of layer j, g the gravitional acceleration, and t_j is the thickness of the layer j.